NAVAL POSTGRADUATE SCHOOL

Monterey, California

THESIS

GENERATION OF THE AMBIGUITY FUNCTION FOR ULTRA WIDEBAND RADAR WAVEFORMS

by

Efrain Leon

December, 1993

Thesis Advisor: Gurnam Gill

Thesis Co-Advisor: Darwish Mohamed

DISCLAIMER NOTICE

THIS DOCUMENT IS BEST QUALITY AVAILABLE. THE COPY FURNISHED TO DTIC CONTAINED A SIGNIFICANT NUMBER OF COLOR PAGES WHICH DO NOT REPRODUCE LEGIBLY ON BLACK AND WHITE MICROFICHE.

REPORT DOCUMENTATION PAGE

Form Approved
OMB No. 0704-0188

1. AGENCY USE ONLY (*Leave Blank*)	2. REPORT DATE	3. REPORT TYPE AND DATES COVERED
	December 17, 1993	Master's Thesis

4. TITLE AND SUBTITLE

GENERATION OF THE AMBIGUITY FUNCTION FOR ULTRA WIDEBAND RADAR WAVEFORMS

5. FUNDING NUMBERS

6. AUTHOR(S)

Leon, Efrain

7. PERFORMING ORGANIZATION NAMES (S) AND ADDRESS(ES)

Naval Postgraduate School
Monterey, CA 93943-5000

8. PERFORMING ORGANIZATION

9. SPONSORING/MONITORING AGENCY NAME(S) AND ADDRESS(ES)

Naval Postgraduate School
Monterey, CA 93943-5000

10. SPONSORING/MONITORING AGENCY REPORT NUMBER

11. SUPPLEMENTARY NOTES The views expressed in this thesis are those of the author and do not reflect the official policy or position of the Department of Defense or the U.S. Government.

12a. DISTRIBUTION/AVAILABILITY STATEMENT

Approved for public release; distribution is unlimited.

12b. DISTRIBUTION CODE

13. ABSTRACT (*Maximum 200 words*)

The Ambiguity Function is one of the tools used to study the suitability of waveforms for radar applications. An understanding of this function gives the radar engineer an insight into different radar waveforms and permits him to select the best design for a particular system application. This thesis investigates the Ambiguity Function for ultra wideband radar waveforms generated by the Fourier Synthesis Method, which provides the capability to produce very narrow pulses in a coherent and controllable form. Since, for ultra wideband radar waveforms, the transmitted signal is a baseband signal without sinusoidal carrier, the Ambiguity Function for this kind of waveform should be generated by Doppler processing in the time domain rather than in the frequency domain, as is done for conventional radar waveforms. In this thesis, the Ambiguity Function has been generated and analyzed for two different ultra wideband radar waveforms by means of computer simulation of a radar receiver which incorporates time-Doppler processing.

14. SUBJECT TERMS

16. PRICE CODE

15. NUMBER OF PAGES 84

17. SECURITY CLASSIFICATION OF REPORT	18. SECURITY CLASSIFICATION OF THIS PAGE	19. SECURITY CLASSIFICATION OF ABSTRACT	20. LIMITATION OF ABSTRACT
UNCLASSIFIED	UNCLASSIFIED	UNCLASSIFIED	UNLIMITED

NSN 7540-01-280-5500

Standard Form 298 (Rev. 2-89)
Prescribed by ANSI Std. 239-18, 298-102

Approved for public release; distribution is unlimited.

GENERATION OF THE AMBIGUITY FUNCTION FOR ULTRAWIDEBAND RADAR WAVEFORMS

by

Efrain Leon
Lieutenant Commander, Venezuelan Navy
B.S., Venezuelan Naval Academy, 1982

Submitted in partial fulfillment
of the requirements for the degree of

MASTER OF SCIENCE IN ELECTRICAL ENGINEERING

from the

NAVAL POSTGRADUATE SCHOOL
December, 1993

Author: 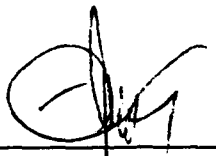
Efrain Leon

Approved By: 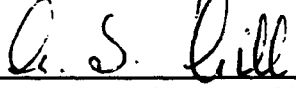
Dr. Gurnam Gill, Thesis Advisor


Dr. Darwish Abdel Aziz Mohamed, Thesis Co-Advisor

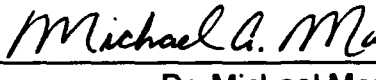
Dr. Michael Morgan, Chairman
Department of Electrical and Computer Engineering

ABSTRACT

The Ambiguity Function is one of the tools used to study the suitability of waveforms for radar applications. An understanding of this function gives the radar engineer an insight into different radar waveforms and permits him to select the best design for a particular system application. This thesis investigates the Ambiguity Function for ultra wideband radar waveforms generated by the Fourier Synthesis Method, which provides the capability to produce very narrow pulses in a coherent and controllable form. Since, for ultra wideband radar waveforms, the transmitted signal is a baseband signal without sinusoidal carrier, the Ambiguity Function for this kind of waveform should be generated by Doppler processing in the time domain rather than in the frequency domain, as is done for conventional radar waveforms. In this thesis, the Ambiguity Function has been generated and analyzed for two different ultra wideband radar waveforms by means of computer simulation of a radar receiver which incorporates time-Doppler processing.

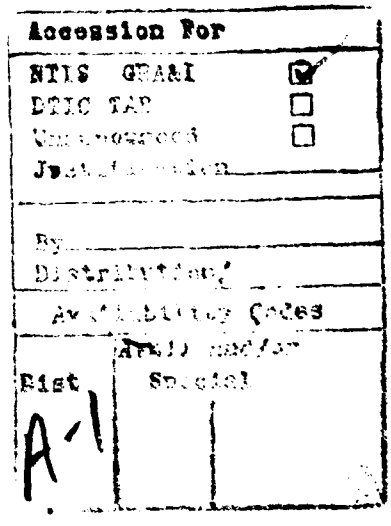

CONTENTS

LIST OF FIGURES

ACKNOWLEDGEMENT

I want to dedicate this work to my wife Jacqueline and to my children, Ernesto, Barbara, and Paula. The patience, understanding, and sacrifice which they have offered during my course of study at the NPS are valuable beyond measure, and I will always be grateful. Additionally, I would like to express my sincere appreciation to Fred Levien, Donald Wadsworth, and Darwish Abdel Aziz Mohamed, all professors at NPS, for their kind and diligent efforts in helping me to complete this work.

I. INTRODUCTION

A. OVERVIEW

The Ambiguity Function is one of the most important tools used to study the suitability of waveforms for radar applications. An understanding of this function gives the radar engineer an insight into waveform performance and permits him to select the most useful waveform for the specific application. This thesis investigates the Ambiguity Function for ultra wideband (UWB) radar waveforms generated by the Fourier Synthesis Method (FSM) [Ref. 1]. This method consists of adding several sinusoidal sources to produce very narrow pulses and offers several advantages. For instance, very short pulses can be generated in a coherent and controllable fashion. Also, lower power sources and lower switching speeds can be used. Thus, the FSM can mitigate the high peak power problem often encountered in UWB radar waveforms.

This thesis consists of four chapters. Chapter I is a brief introduction to UWB radar technology, and makes a summary of the most relevant problem areas that need to be addressed before considering UWB radar as a practical and useful tool. Chapter II presents the concept of the Ambiguity Function and provides mathematical expressions for narrowband and wideband cases. In addition, it defines the Ambiguity Function used in this thesis for UWB radar waveforms. Chapter III details the computation of the Ambiguity Function by computer simulation of two UWB radar waveforms: a train of

baseband pulses produced with the FSM; and a pulse train of Barker code of length 13. Conclusions and recommendations are offered in Chapter IV. Finally, Appendix A discusses the Fourier Synthesis Method and Appendix B contains simulation programs written in MATLAB, which are used for the waveforms presented in Chapters II and III.

B. ULTRA WIDEBAND RADAR

Although UWB radar technology has only recently drawn widespread attention, it dates back more than 30 years, when in 1960 John C. Cook proposed a single-cycle VHF radar for measuring the thickness of ice. Later, UWB technology was applied in the remote sensing area, specifically for subsurface probing in the detection of buried pipes, mines and tunnels [Ref. 2]. UWB technology is widely used in this area to this day.

One definition of UWB radar specifies a signal bandwidth greater than 25 percent of the center frequency, where percent bandwidth (also known as relative bandwidth) is defined as 100 times the absolute bandwidth divided by the center frequency [Ref. 1].

UWB technology can be and has been applied to many areas of technology. In the field of communications, there are UWB applications related to spread spectrum systems. In weapons systems applications, UWB has been found to cause target damage by generating extreme field strengths, thereby causing disruption of the target's electronic systems. The most recent developments in the weapons area have been due to advances in high-powered microwave generation. In the area of radar, the UWB term is applied to systems which are also known as carrier-free or baseband or non-sinusoidal or impulse

radars. In the case of radar applications, work has been concentrated in the area of ground probing systems. More recently, perimeter security systems have also been tested. These security systems exploit the excellent range-resolution made possible by short pulses, thereby permitting short-range detection of intruders [Ref. 2].

Application of UWB technology in radar systems has recently attracted attention because of several factors:

- Extremely wide bandwidth improves target identification abilities
- A pulsewidth which is shorter than the target dimensions enhances the study of transient scattering
- Improved penetration of foliage and camouflage
- Greater potential in defeating radar absorbing materials and shaping of "stealthy" targets

Furthermore, the widely accepted use of UWB radar as a tool for underground probing is also a motivation for more investigation and understanding of UWB radar technology [Ref. 1].

In spite of all these potential UWB radar capabilities, there are problems that must be addressed before the technology can be applied to practical purposes. For example,

- The laws of physics dictate that for the same pulse repetition frequency, the shorter the pulse, the greater must be the peak power in order to have the same energy in every pulse. Since UWB radar uses a pulsewidth as short as 1 or 0.1 nsec, the corresponding peak power must be much greater than that of conventional radars in

order to achieve the same energy on target. However, the high-power transmitter technology needed to provide the large pulse energies for UWB radars is for the most part still in the experimental phase.

- Fast Analog-to-Digital converters for digital implementation of UWB radar are not generally available for real time applications. To circumvent this problem, UWB radars for ground probing applications have used sampling oscilloscopes connected to antennas to collect return signals. Oscilloscopes are adequate for experimental work, but they are not appropriate for operational radars.
- There is an additional problem in the phenomenon of receiver burnout at high peak power when using a single antenna, and also the availability of UWB duplexers is generally low.
- The lack of high gain-aperture product antennas has also impeded the development of high-performance (long-range) UWB radars.

One way to increase the gain in low-gain antennas is to combine them in a phased array. This would provide results consistent with a high-gain antenna. However, a disadvantage to this approach is that phased arrays generally have poor sidelobes when operated over wide bandwidth.

UWB radar is a technology that is still under development and is fundamentally different from conventional radars. Thus, there is a lack of methods for analysis, which must be developed in order to gain a better understanding of its potential military

applications in such areas as detection of low radar-cross-section targets and noncooperative target recognition.

II. THE AMBIGUITY FUNCTION

This chapter describes the radar Ambiguity Function and presents mathematical expressions for narrowband and wideband cases. Properties of the Ambiguity Function are addressed and the definition of the Ambiguity Function used in this thesis for UWB radar waveforms is developed.

A. AMBIGUITY FUNCTION

The Ambiguity Function is the output response of a matched radar receiver to a single point target at all possible combinations of ranges and velocities [Ref. 3]. It dates back 40 years, and was first defined by Woodward as a mathematical funtion for computing the output response of a matched filter to a range-delayed, Doppler-shifted radar signal [Ref. 4].

The Ambiguity Function provides an indication of the limitations and utility of particular classes of radar waveforms, and gives the radar designer general guidelines for the selection of suitable waveforms for various applications [Ref. 5]. For example, if precise measurements of both the range and Doppler of an echo source are required, the ideal waveform would have an Ambiguity Function consisting of a single peak at the origin, sufficiently thin in both dimensions to achieve the desired resolution. The Ambiguity Function is also used to assess the properties of the transmitted waveform

with regard to its target resolution, measurement accuracy, ambiguity, and response to clutter.

Depending upon the bandwidth of the transmitted signal, the resulting Ambiguity Function has different names. Thus, if the signal used by the radar is confined to a small band of frequencies around a large carrier frequency, its Ambiguity Function will be called the *Narrowband Ambiguity Function.* On the other hand, if the signal occupies a large band in the frequency spectrum (as in the case of ultra wideband radar signals) and is no longer confined to a small band of frequencies, the corresponding Ambiguity Function will be called the *Wideband Ambiguity Function.*

B. MATHEMATICAL EXPRESSION FOR NARROWBAND AMBIGUITY FUNCTION

The narrow-band Ambiguity Function of a pulsed carrier signal is derived as follows [Ref. 6]:

A narrow bandpass signal can be represented as

$$s(t) = g(t)\cos(\omega_c t + \phi(t)), \tag{2.1}$$

where $g(t)$ is the natural envelope of $s(t)$ and $\phi(t)$ is the phase of $s(t)$.

Expressing Equation (2.1) in terms of both sines and cosines, it can be rewritten as

$$s(t) = g_c(t)\cos\omega_c t - g_s(t)\sin\omega_c t, \tag{2.2}$$

where

$$g_c(t) = g(t)\cos\phi(t) \tag{2.3}$$

and

$$g_s(t) = g(t)\sin\phi(t) \tag{2.4}$$

are known as in-phase and quadrature components of the signal.

Let

$$u(t) = g_c(t) + jg_s(t). \tag{2.5}$$

This expression is the complex envelope of signal $s(t)$. Expressing $s(t)$ in terms of the complex envelope $u(t)$ can be accomplished by multiplying Equation (2.5) by exponential terms,

$$u(t)e^{j\omega_c t} = u(t)[\cos\omega_c t + j\sin\omega_c t] \quad . \tag{2.6}$$

Using Equation (2.5) in (2.6) a final expression can be obtained for $s(t)$ in terms of the complex envelope $u(t)$:

$$s(t) = \mathrm{Re}[u(t)e^{j\omega_c t}]. \tag{2.7}$$

Taking into account the equations described earlier, signal $s(t)$ can be represented as

$$s(t) = \tfrac{1}{2}u(t)e^{j\omega_c t} + \tfrac{1}{2}u^*(t)e^{j\omega_c t}. \tag{2.8}$$

The output of a filter is defined as the convolution between the input signal and the impulse response of the filter, or

$$S_{out}(t) = \int_{-\infty}^{\infty} s(\lambda)h(t-\lambda)d\lambda, \tag{2.9}$$

where

$$h(t) = Ks^*(t_1 - t) \tag{2.10}$$

is the impulse response of a matched filter and t_1 is the time delay affecting the input signal.

Using Equation (2.10) in (2.9) yields

$$S_{out}(t) = K\int_{-\infty}^{\infty} s(\lambda)s^*(\lambda-(t-t_1))d\lambda. \tag{2.11}$$

Inserting (2.8) in (2.11) produces

$$S_{out}(t) = \tfrac{1}{4}K\int_{-\infty}^{\infty}[u(\lambda)e^{j\omega_c\lambda} + u^*(\lambda)e^{-j\omega_c\lambda}]$$

$$[u^*(\lambda-t+t_1)e^{-j\omega_c(\lambda-t+t_1)} + u(\lambda-t+t_1)e^{j\omega_c(\lambda-t+t_1)}]d\lambda \ . \tag{2.12}$$

Expanding Equation (2.12) yields

$$S_{out}(t) = \tfrac{1}{4}Ke^{j\omega_c(t-t_1)}\int_{-\infty}^{\infty} u(\lambda)u^*(\lambda-t+t_1)d\lambda +$$

$$\tfrac{1}{4}Ke^{-j\omega_c(t-t_1)}\int_{-\infty}^{\infty} u^*(\lambda)u(\lambda-t+t_1)d\lambda +$$

$$\tfrac{1}{4}Ke^{j\omega_c(t-t_1)}\int_{-\infty}^{\infty} u^*(\lambda)u^*(\lambda-t+t_1)e^{-j2\omega_c\lambda}d\lambda +$$

$$\tfrac{1}{4}Ke^{-j\omega_c(t-t_1)}\int_{-\infty}^{\infty} u(\lambda)u(\lambda-t+t_1)e^{j2\omega_c\lambda}d\lambda. \tag{2.13}$$

From the above result it can be noted that the first two terms are complex conjugates of each other, and so are the last two terms. As a consequence, Equation (2.13) can be rewritten as

$$S_{out}(t) = \tfrac{1}{2}KRe[e^{j\omega_c(t-t_1)}\int_{-\infty}^{\infty} u(\lambda)u^*(\lambda-t+t_1)d\lambda] +$$

$$\frac{1}{2}KRe[e^{j\omega_c(t-t_1)}\int_{-\infty}^{\infty} u^*(\lambda)u^*(\lambda-t+t_1)e^{-j2\omega_c\lambda}d\lambda]. \quad (2.14)$$

The integral of the second term in Equation (2.14) is defined as the Fourier Transform of the product of $u^*(\lambda)$ and $u^*(\lambda-t+t_1)$ centered at $2\omega_c$. This means that the second term of Equation (2.14) need not be considered, because it is dealing with narrowband bandpass signals whose Fourier Transform is limited to a frequency centered at ω_c. As a consequence, Equation (2.14) can be rewritten

$$S_{out}(t) = \frac{1}{2}KRe[e^{j\omega_c(t-t_1)}\int_{-\infty}^{\infty} u(\lambda)u^*(\lambda-t+t_1)d\lambda]. \quad (2.15)$$

Furthermore, the above equation can also be expressed as

$$S_{out}(t) = Re[u_{out}(t)e^{j\omega_c t}] \ , \quad (2.16)$$

where

$$u_{out}(t) = \frac{1}{2}Ke^{-j\omega_c t_1}\int_{-\infty}^{\infty} u(\lambda)u^*(\lambda-t+t_1)d\lambda. \quad (2.17)$$

Thus, Equations (2.16) and (2.17) state that the output signal of the matched filter $S_{out}(t)$ has a complex envelope u_{out} which would have been obtained if the envelope had been passed through a filter that was matched to it. Furthermore, using $t_1 = 0$ and $K = 2$ in Equation (2.17) yields

$$u_{out}(t) = \int_{-\infty}^{\infty} u(\lambda)u^*(\lambda-t)d\lambda. \quad (2.18)$$

Assuming received signal is Doppler-shifted by f_d, Equation (2.18) can be written as

$$u_{out}(t, f_d) = \int_{-\infty}^{\infty} u(\lambda)e^{j2\pi f_d\lambda}u^*(\lambda-t)d\lambda. \quad (2.19)$$

Reversing the roles of λ and t, and assigning the symbol χ to u_{out}, Equation (2.19) can be expressed in the standard notation as

$$\chi(\lambda, f_d) = \int_{-\infty}^{\infty} u(t)u^*(t-\lambda)e^{j2\pi f_d t}dt. \qquad (2.20)$$

The magnitude of the complex envelope $|\chi(\lambda, f_d)|$ is called the *Narrowband Ambiguity Function*, even though some authors define it as the square of the magnitude of complex envelope (i.e., $|\chi(\lambda, f_d)|^2$). In this thesis the Narrowband Ambiguity Function is defined as the absolute value of the envelope of the output of a matched filter when the input to the filter is a Doppler-shifted version of the original signal to which the filter was matched [Ref. 6]. Its mathematical expression is written as

$$|\chi(\lambda, f_d)| = \left| \int_{-\infty}^{\infty} u(t)u^*(t-\lambda)e^{j2\pi f_d t}dt \right| \qquad (2.21)$$

From the above equation it is noticeable that the two parameters of the Narrowband Ambiguity Function are a delay λ and a frequency shift f_d. $|\chi(0,0)|$ is interpreted as the output when the input signal is returned from a point target at the delay and frequency shift for which the matched filter was designed. A positive value of λ, indicates a target beyond the reference delay λ and a positive value of f_d indicates an incoming target.

C. THE WIDEBAND AMBIGUITY FUNCTION

In contrast to narrowband signals, an immediate consequence of wideband signals is that the effect of target velocity can no longer be approximated by a simple shift in

frequency. The real meaning of the Doppler effect is a compression (or expansion) of the signal, mathematically described by a scale factor in time. The new version of Equation (2.21) takes into account the Doppler scaling factor, and is known as the *Wideband Ambiguity Function.* The most widely accepted version of the Wideband Ambiguity Function was introduced by Kelly and Wishner in their paper "Matched-filter theory for high-velocity accelerating targets" published in 1965 [Ref. 7].

Specifically, the Wideband Ambiguity Function describes the response of a matched filter receiver to all possible delayed and Doppler compressed or expanded versions of the transmitted signal [Ref. 8]. In other words, the Wideband Ambiguity Function states the capability of a radar system to recognize a time-scaled version of the transmitted signal in order to resolve targets based on their differences in range and velocity.

D. MATHEMATICAL EXPRESSION FOR WIDEBAND AMBIGUITY FUNCTION

The Ambiguity Function has been defined as the cross-correlation function between the radar's transmitted signal and the delayed received signal, which has gone through Doppler frequency shift. Since for the ultra wideband case the transmitted signal is a baseband signal, the concept of frequency shift no longer applies. The returned signal should therefore be treated in the time domain. Doppler effect in the time domain is represented by scale factor α rather than frequency shift f_d , and is given by $c+v/c-v$.

When the absolute value of v is small with respect to c (as it is in the case of radar), the approximation $\alpha = 1 + 2v/c$ can be used, where v is the target radial velocity (positive for opening targets, negative for closing targets). The Wideband Ambiguity Function is thus defined [Ref. 8] as

$$\chi(\lambda, \alpha) = \sqrt{\alpha} \int_{-\infty}^{\infty} u(\alpha t) u^*(t - \lambda) dt, \tag{2.22}$$

where $\sqrt{\alpha}\, u(\alpha t)$ represents the energy-normalized received signal. Equation (2.22) defines the Wideband Ambiguity Function as the function of two parameters: the time delay λ and the Doppler scaling factor α, which acts as a time compression or expansion factor in the received radar signal, depending upon the radial velocity of the target.

E. AMBIGUITY FUNCTION OF A UWB RADAR WAVEFORM

An important characteristic of baseband radar waveforms is that the Doppler effect can no longer be approximated as a frequency translation because they do not have any sinusoidal carrier. Therefore, the Doppler effect should be analyzed as a scale factor on the time variable which compresses or expands the received radar waveform. However, this variation in time is so small that it is not possible to notice it in a single radar pulse. The analysis of UWB radar waveforms include the complete waveform, involving a number of pulses rather than a single pulse [Ref. 9]. Thus, in this section, the Ambiguity Function of the time domain Doppler processor, which processes a block of N pulses, is derived [Ref. 9,10].

1. Doppler Effect

Assuming a radar transmits a sequence of N pulses at the time t = 0, T, 2T,... , and each pulse represented by f(t), the transmitted signal can be expressed as a sum of N pulses, as follows

$$S_t(t) = \sum_{i=1}^{N} f[t - (i-1)T] \tag{2.23}$$

Considering the round trip delay of the ith returned pulse as t_i, the received signal can be written as

$$S_r(t) = \sum_{i=1}^{N} f[t - t_i - (i-1)T] \tag{2.24}$$

Considering a target with constant relative velocity v, the range corresponding to the first received pulse can be expressed as

$$R_1 = \frac{c}{2}t_1 \tag{2.25}$$

where t_1 is the round trip delay time of the received signal. Similarly, the range corresponding to the second received pulse becomes

$$R_2 = \frac{c}{2}t_1 + vT \tag{2.26}$$

$$= \frac{c}{2}(t_1 + 2\frac{v}{c}T) = \frac{c}{2}t_2$$

where $t_2 = t_1 + 2\frac{v}{t}T$ represents the round trip delay time for the second received pulse.

Thus, the round trip delay time for the ith pulse can be generalized as

$$t_i = t_1 + 2(i-1)\frac{v}{c}T. \qquad (2.27)$$

Figure 2.1 depicts the timing of pulses using the usual convention that the velocity v of an approaching target is negative since the distance decreases.

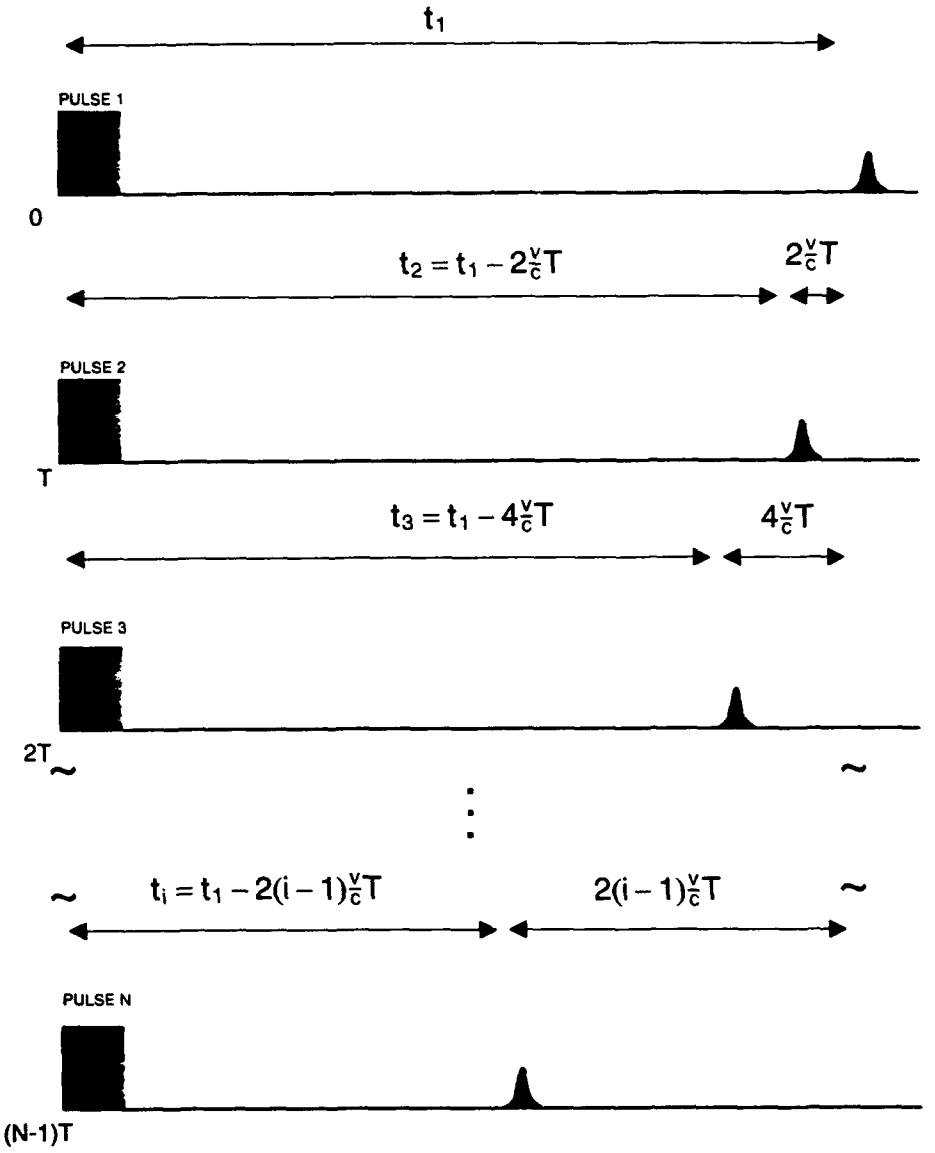

Figure 2.1. Received Signal from an Incoming Target with Constant Relative Velocity v, due to N Radar Transmitted Pulses (i=1,2,3,...N).

The difference between two consecutive round trip delay times t_i and t_{i-1} yields

$$t_i - t_{i-1} = 2\frac{v}{c}T = \psi_r \ . \tag{2.28}$$

Using Equation (2.28) in (2.27), the round trip delay of the ith pulse can be written as

$$t_i = t_1 + (i-1)\psi_r \qquad \text{for i=1,2,...,N pulse.} \tag{2.29}$$

Substituting the above expression for t_i in Equation (2.24) yields

$$S_r(t) = \sum_{i=1}^{N} f[t - t_1 - (i-1)(T + \psi_r)]. \tag{2.30}$$

Comparison of Equations (2.23) and (2.30) shows that the pulse repetition interval (T_r) of the received signal from a moving target is given by

$$T_r = T + \psi_r = T(1 + 2\frac{v}{c}) = \alpha T \tag{2.31}$$

where α is the Doppler scaling factor affecting the time interval T of the waveform.

Equation (2.31) represents the Doppler effect. According to this equation, the Doppler effect changes the duration of the received signal with respect to the transmitted waveform.

2. Matched Filtering

Individual pulses are detected with a matched filter before the Doppler processing is performed. The output of a matched filter due to sequence of incoming pulses is given by

$$g(t) = \sum_{i=1}^{N} C[t - t_1 - (i-1)(T + \psi_r)] \tag{2.32}$$

where C(t) is the autocorrelation function of pulse shape f(t).

As an example, consider an input consisting of a train of rectangular pulses of width τ and time interval $T + \psi_r$. The output of a matched filter becomes a train of triangular pulses with width 2τ separated by $T + \psi_r$, as shown in Figure 2.2.

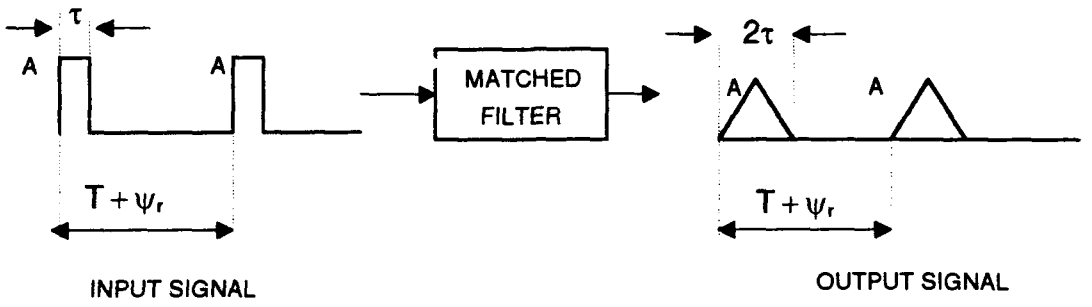

Figure 2.2. Principle of Correlation Detection Implemented by a Matched Filter.

3. Doppler Processing Technique

The Doppler effect produced by a moving target may be used in a UWB radar to determine its relative velocity. It also distinguishes moving targets from stationary targets. The principle of a Doppler processor is shown in Figure 2.3. The Doppler processor is basically a feedback circuit with variable delay where an adder adds the delayed signal to the input signal.

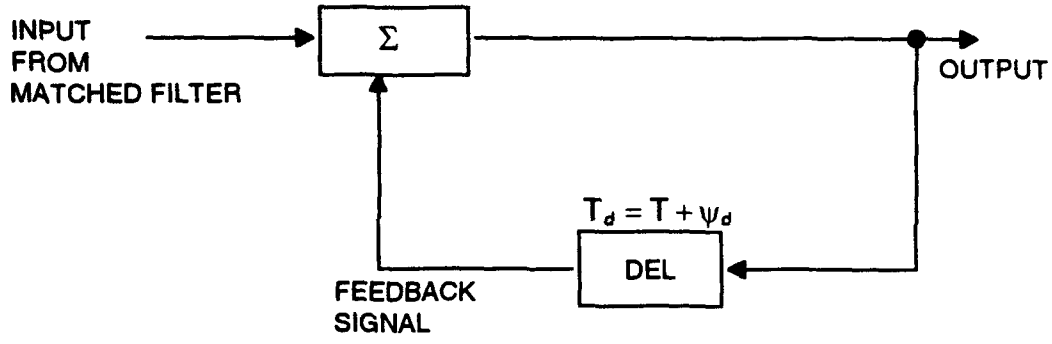

Figure 2.3. Doppler Processor Based on Feedback Delay Circuit.

In order to understand this device, consider the general case where the delay circuit is set for the delay $T_d = T + \psi_d$ but the target has the Doppler time ψ_r due to its velocity ($\psi_r = 2\ v/c\ T$). There is a difference $\Delta\psi$ between the Doppler time ψ_d of the processor and the Doppler time ψ_r of the signal ($\Delta\psi = \psi_d - \psi_r$). Considering that the output of the matched filter is a train of 3 triangular pulses ($N = 3$) separated by a time interval $T + \psi_r$, the output of the Doppler processor when $\Delta\psi = 0$ will be a correlation function centered at $(N-1)(T+\psi_r) + \tau$. The output of the same Doppler processor when $\Delta\psi = \pm\tau, \pm 2\tau$, will be correlation functions centered at $(N-1)(T+\psi_r) + \tau$, $(N-1)(T+\psi_r) + \tau \pm \Delta\psi$ and $(N-1)(T+\psi_r) + \tau \pm 2\Delta\psi$. This concept is illustrated in Figure 2.4.

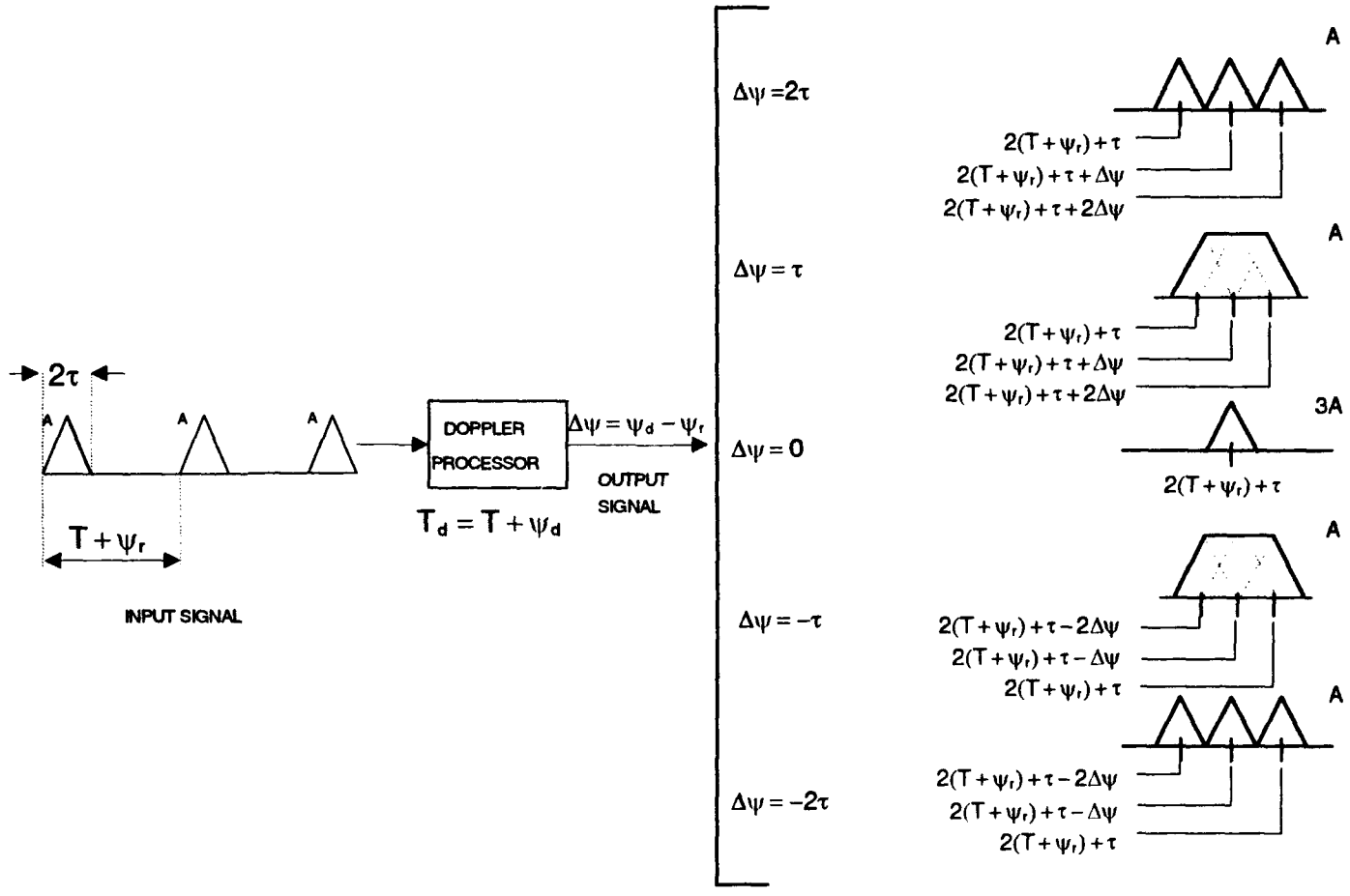

Figure 2.4. Output of the Doppler Processor for Five Values of the Doppler Time Difference $\Delta\psi$.

Output of the Doppler processor can be written as

$$D_{out}(t, \Delta\psi) = C[t - t_1 - (N-1)(T + \psi_r) + \tau]$$

$$+C[t - t_1 - (N-1)(T + \psi_r) + \tau + \Delta\psi] + \ldots$$

$$\ldots + C[t - t_1 - (N-1)(T + \psi_r) + \tau + (N-1)\Delta\psi]$$

$$= \sum_{k=1}^{N} C[t - t_1 - (N-1)(T + \psi_r) + \tau + (k-1)\Delta\psi] \qquad (2.33)$$

Substituting $t - t_1 - (N-1)(T + \psi_r) + \tau$ with t (in order to shift the distance to the point target to zero) and after normalizing the function by the factor 1/N (to obtain a peak output signal equal to one), Equation (2.33) can be expressed as

$$D_{out}(t, \Delta\psi) = \frac{1}{N} \sum_{k=0}^{N-1} C[t + k\Delta\psi], \qquad (2.34)$$

which expresses the output of the Doppler processor as the sum of the N correlation functions C(t) as function of the Doppler time difference $\Delta\psi$.

4. Ambiguity Function of UWB Processor

Equation (2.34) relates the output of a matched filter with the time delay and time Doppler. It also represents the Ambiguity Function of the train of UWB radar pulses. Taking the absolute value of Equation (2.34) and replacing D_{out} with χ and t with λ, Equation (2.34) can be rewritten in terms of Ambiguity Function as

$$|\chi(\lambda, \Delta\psi)| = |\frac{1}{N} \sum_{k=0}^{N-1} C(\lambda + k\Delta\psi)| \qquad (2.35)$$

A block diagram of the UWB radar processor is shown in Figure 2.5. The function of the processor is summarized in the following steps: (1) The signal returned from a target is passed through a matched filter for selective reception and noise suppression, and (2) the output of the matched filter is passed through a bank of Doppler processors set to different time delays ($T_d = T + \psi_d$).

A computer simulation of the block diagram of Figure 2.5 is used to compute the Ambiguity Function

$$|\chi(\frac{\lambda}{\tau}, \frac{\Delta\psi}{\tau})| = |\frac{1}{N}\sum_{k=0}^{N-1} C(\frac{\lambda}{\tau} + k\frac{\Delta\psi}{\tau})|, \tag{2.36}$$

which was obtained by normalizing Equation (2.35) by the pulsewidth τ.

As an example, Figure 2.6 shows the UWB Ambiguity Function of Equation (2.36) for a received signal shown in Figure 2.5, where N=4 rather than N=2. The UWB Ambiguity Function shown in Figure 2.6 is a three-dimensional surface as a function of normalized time delay (λ/τ) and normalized Doppler shift ($\Delta\psi/\tau$), where the former represents range and the latter represents velocity. The relative velocity v is obtained from $\Delta\psi/\tau$ axis using the equation

$$v = \frac{\Delta\psi}{2T}c \tag{2.37}$$

It should be noted that as N increases, the sidelobes of the function given by Equation (2.35) decreases, which is a desired feature in order to obtain better velocity resolution [Ref. 9,10].

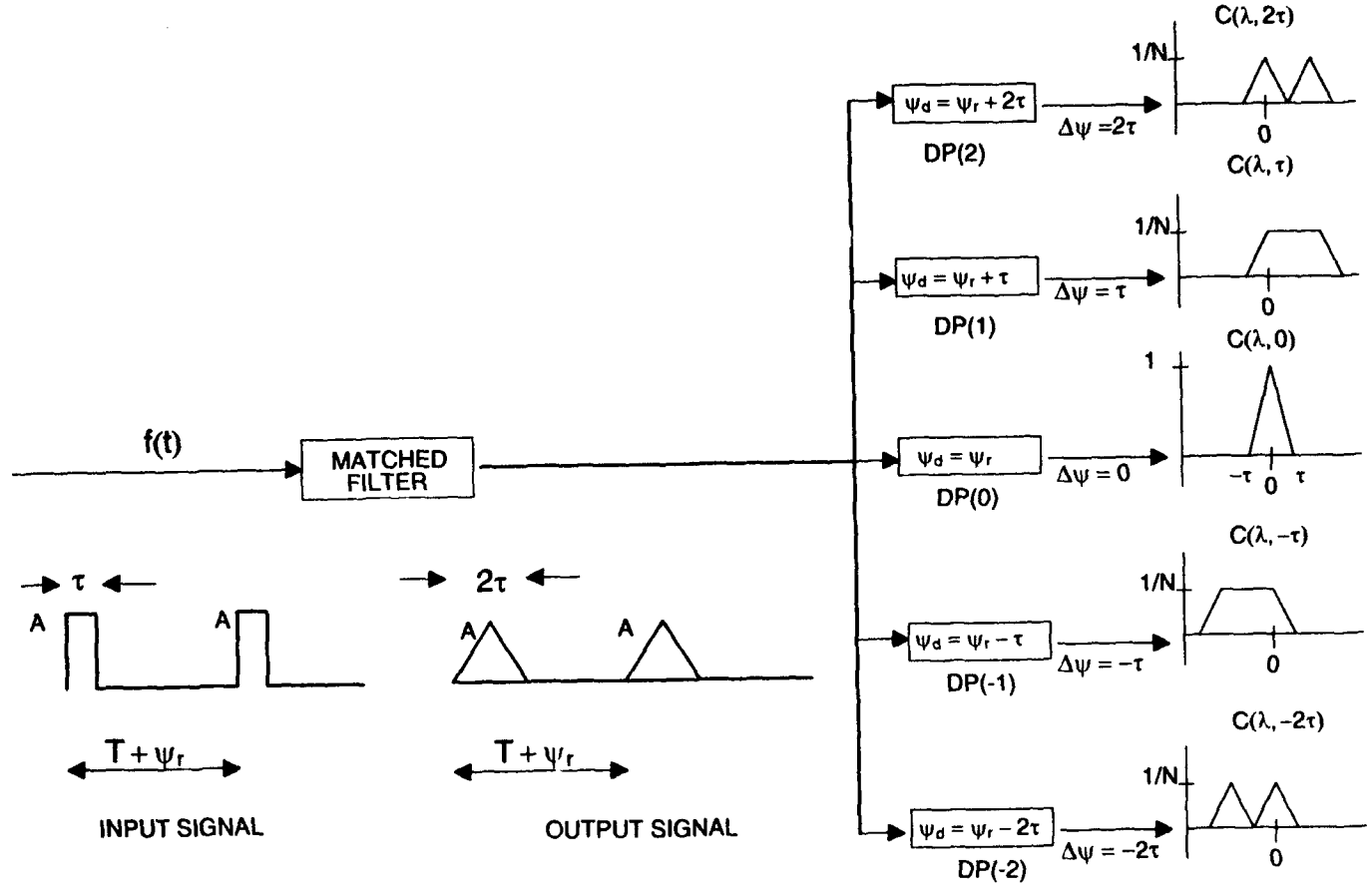

Figure 2.5. Block Diagram of Radar Processor Considering Rectangular Pulses as Received Signal. The Whole Processor Consists of a Matched Filter and Doppler Processor Bank.

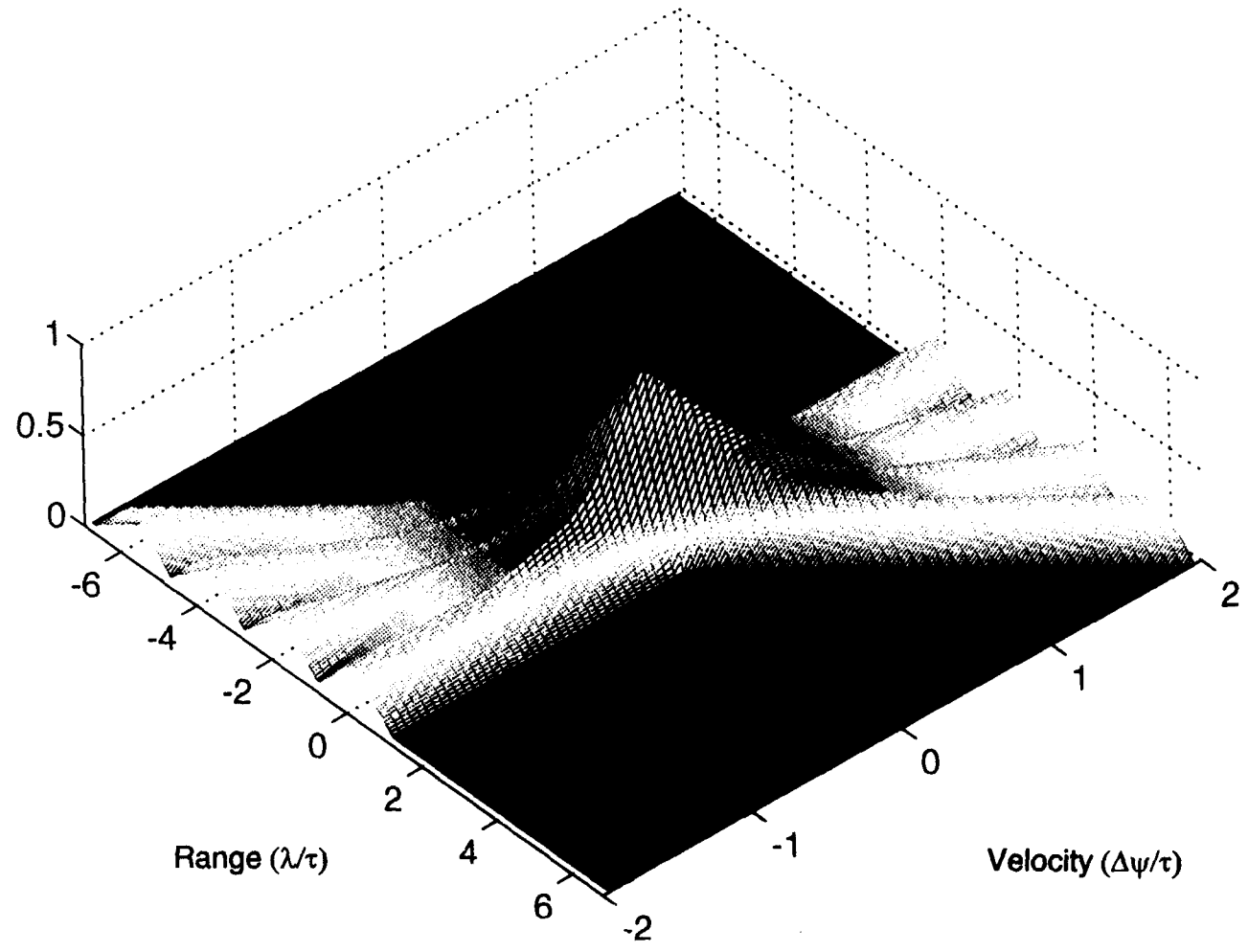

Figure 2.6. The Ambiguity Function of a Train of 4 UWB Rectangular Pulses.

F. IMPORTANT PROPERTIES OF THE AMBIGUITY FUNCTION

Assuming that the radar signal has a unit energy, the Ambiguity Function given by Equations (2.21) and (2.35) has the following properties:

1. Property I

$$|\chi(-\lambda, -f_d)| = |\chi(\lambda, f_d)| \quad \text{(Narrowband case)}$$

$$|\chi(-\lambda, -\Delta\psi)| = |\chi(\lambda, \Delta\psi)| \quad \text{(UWB radar case)}$$

The first property states that the Ambiguity Function has a symmetry relation about the origin.

2. Property II

$$|\chi(\lambda, f_d)| \leq |\chi(0, 0)| = 1 \quad \text{(Narrowband case)}$$

$$|\chi(\lambda, \Delta\psi)| \leq |\chi(0, 0)| = 1 \quad \text{(UWB radar case)}$$

This second property states that for normalized signals the maximum value of the Ambiguity Function occurs at the origin and its value at that point is equal to one.

3. Property III

$$\int_{-\infty}^{\infty}\int_{-\infty}^{\infty} |\chi(\lambda, f_d)| d\lambda df_d = \quad \text{(Narrowband case)}$$

$$\int_{-\infty}^{\infty}\int_{-\infty}^{\infty} |\chi(\lambda, \Delta\psi)| d\lambda d\Delta\psi = \quad \text{(UWB radar case)}$$

Property III is known as the *"radar uncertainly principle"* or *"law of the conservation of ambiguity"*. This states that the volume underneath the Ambiguity Function is equal to a constant value of one.

4. Property IV

$$|\chi(\lambda, 0)| = \left| \int_{-\infty}^{\infty} u(t)u^*(t-\lambda)dt \right| = |C(\lambda)| \quad \text{(Narrowband case)}$$

$$|\chi(\lambda, 0)| = \left| \frac{1}{N} \sum_{k=0}^{N-1} C(\lambda) \right| \quad \text{(UWB radar case)}$$

This property states if a cut is made through the time delay axis the Ambiguity Function defines the autocorrelation function of the signal.

G. IDEAL AMBIGUITY FUNCTION

The ideal Ambiguity Function is represented by a single peak of infinitesimal thickness at the origin and being zero everywhere else, as is shown in Figure 2.7a. The single spike implies no ambiguity, and its infinitesimal thickness at the origin allows the echo delay time (λ) and the Doppler variation (f_d or $\Delta\psi$) to be determined at the same time accurately. For this reason this would permit the precise resolution of two targets. However, this kind of Ambiguity Function is impossible to achieve in the real life, so a more realistic approximation of this ideal is used, called the *thumbtack* Ambiguity Function, which is shown in Figure 2.7b. This approximation takes into account the restrictions imposed by the requirements for a fixed value at the origin and a constant volume enclosed under the $|\chi|$ surface. Note that if the peak is made too narrow, the requirements for a constant volume would cause peaks to form in areas others than the origin, generating ambiguities. In other words, the requirements for ambiguity and accuracy in many cases are not possible to achieve simultaneously.

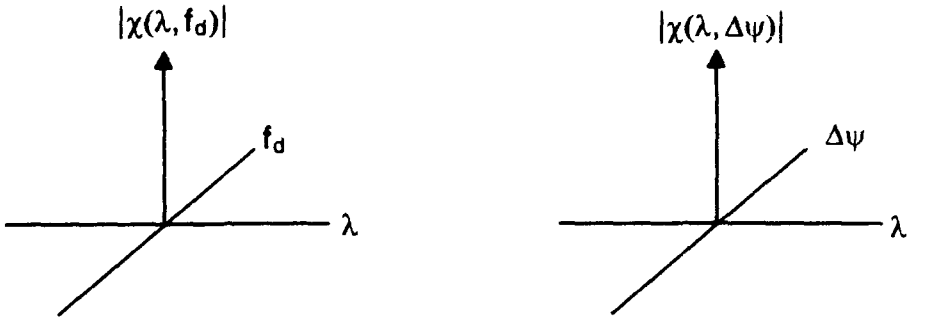

Ideal Narrowband Ambiguity Function

Ideal UWB Ambiguity Function

a)

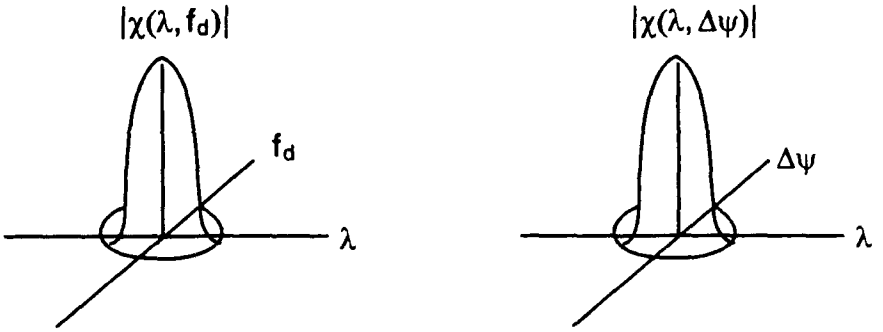

Approximation of Ideal
Narrow Band Ambiguity Function

Approximation of Ideal
UWB Ambiguity Function

b)

Figure 2.7. a). Ideal Ambiguity Function for Narrowband and UWB Cases. b). Approximation of Ideal Ambiguity Function for Narrowband and UWB Cases.

III. AMBIGUITY FUNCTION OF UWB RADAR WAVEFORMS GENERATED BY THE FOURIER SYNTHESIS METHOD

In this chapter Ambiguity Functions are generated and analyzed for two different UWB radar waveforms produced by the Fourier Synthesis Method. The first UWB radar waveform consists of a train of UWB radar pulses generated by using eleven sinusoidal sources, and the second waveform is a pulse train of Barker code of length 13 which is generated by using sixty-five sinusoidal sources.

A computer simulation of the block diagram shown in Figure 3.1 is used to compute the Ambiguity Function given by Equation (2.36), where analysis is done in order to determine the performance and feasibility of the particular waveform.

A. AMBIGUITY FUNCTION OF A TRAIN OF UWB RADAR PULSES

1. Transmitted UWB Waveform

Figure 3.2 shows a radiated waveform consisting of a train of four UWB radar pulses generated by using the FSM with eleven oscillators. Every pulse has width τ and repetition interval T.

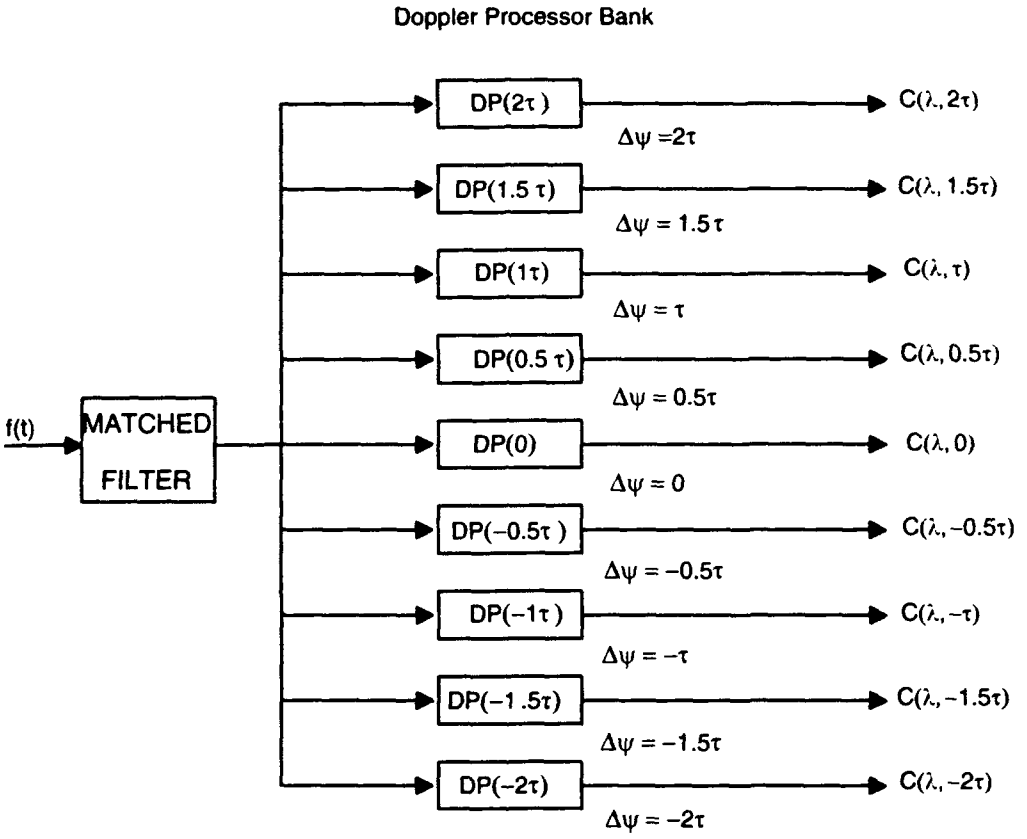

Figure 3.1. Block Diagram of Radar Processor Used in the Computer Simulation.

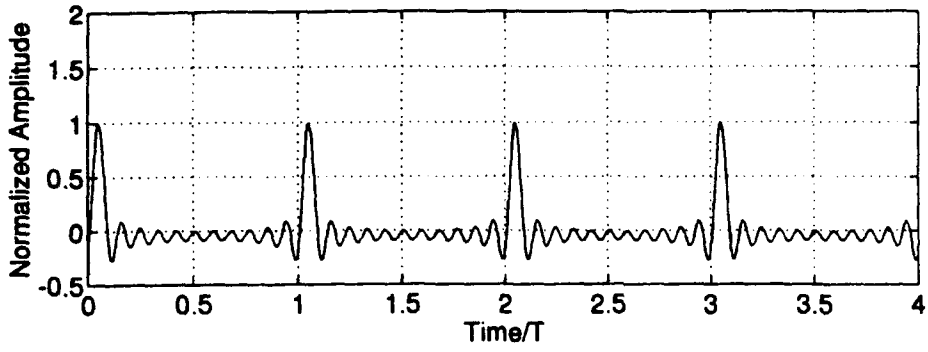

Figure 3.2. Train of 4 UWB Radar Pulses Generated using the FSM with 11 Oscillators.

2. Processing of the Received UWB Signal

A computer simulation of the block diagram in Figure 3.1 is used to obtain outputs of the UWB radar processor. Figure 3.3 shows the output of the matched filter, using as input the waveform given in Figure 3.2.

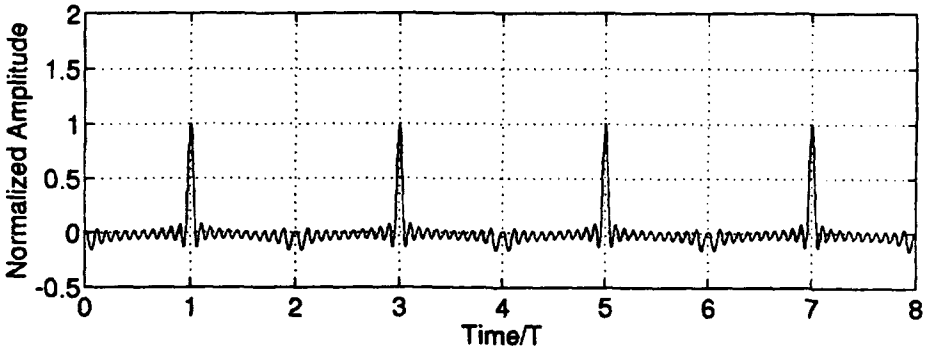

Figure 3.3. Output of Matched Filter for 4 UWB Radar Pulses.

After the matched filtering process has been performed, the signal is passed through a bank of doppler processors. As established earlier, the output of the doppler processor is a function of the doppler time difference $\Delta\psi$. Figure 3.4 shows the output of doppler processor bank for various values of doppler time difference $\Delta\psi$ using four pulses as input ($N = 4$). From this figure it can be seen that the peak amplitude of the output signal is a function of $\Delta\psi$. As $\Delta\psi$ approaches zero, the peak amplitude increases and the duration of the signal decreases.

Computer simulation also shows that for the same doppler time difference $\Delta\psi$, an increasing number of pulses reduce the amplitude of the doppler processor outputs for $\Delta\psi \neq 0$. Figure 3.5 shows the output of the doppler processor bank using sixteen pulses ($N = 16$). Comparing Figures 3.4 and 3.5 it is easy to conclude that as N increases, doppler processor output amplitudes for $\Delta\psi \neq 0$ are reduced.

3. Ambiguity Function

A computer simulation of the block diagram shown in Figure 3.1 is used to compute the Ambiguity Function defined by Equation (2.36). The Ambiguity Function for a train of UWB radar pulses when $N = 4$ is shown in Figure 3.6.

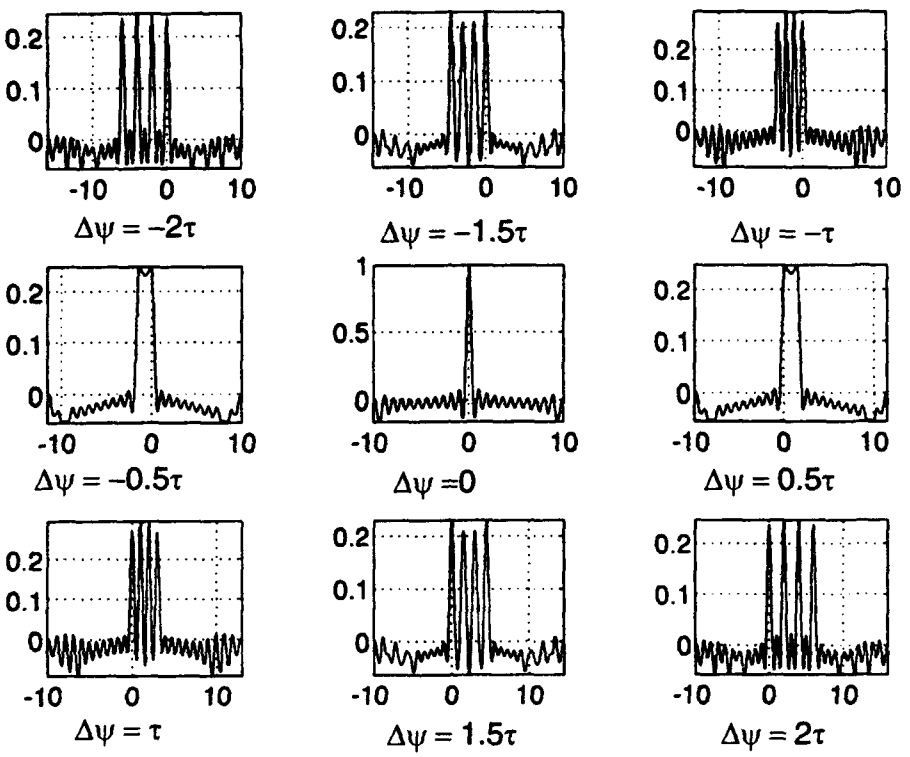

Figure 3.4. Doppler Processor Bank Output for N=4 Pulses (x-axis represents time delay λ/τ and y-axis represents normalized amplitude).

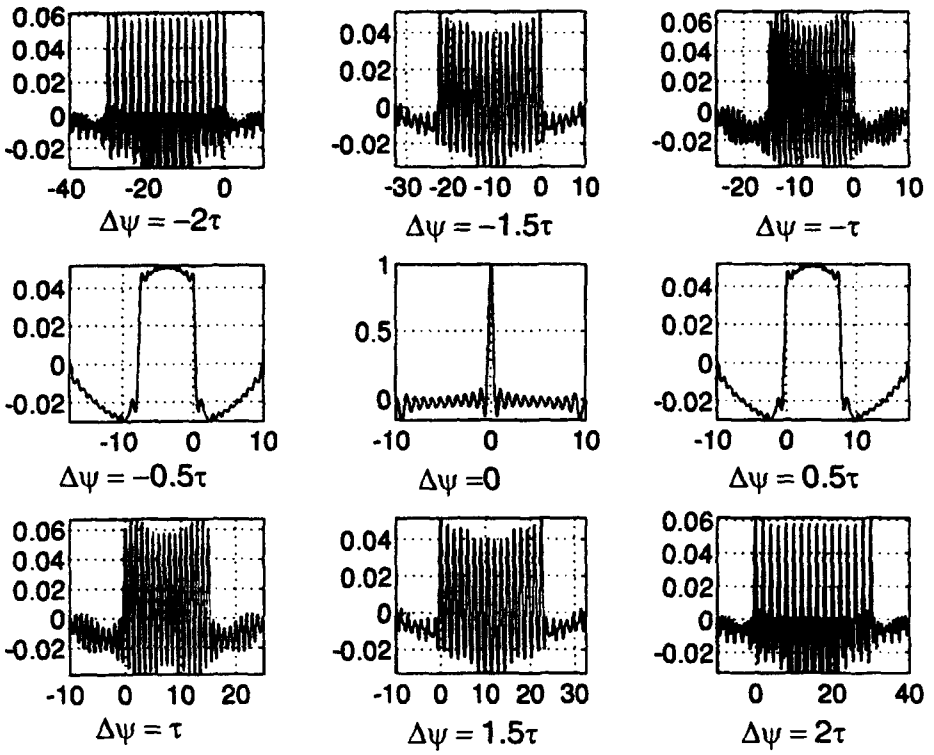

Figure 3.5. Doppler Processor Bank Output for N=16 Pulses (x-axis represents time delay λ/τ and y-axis represents normalized amplitude).

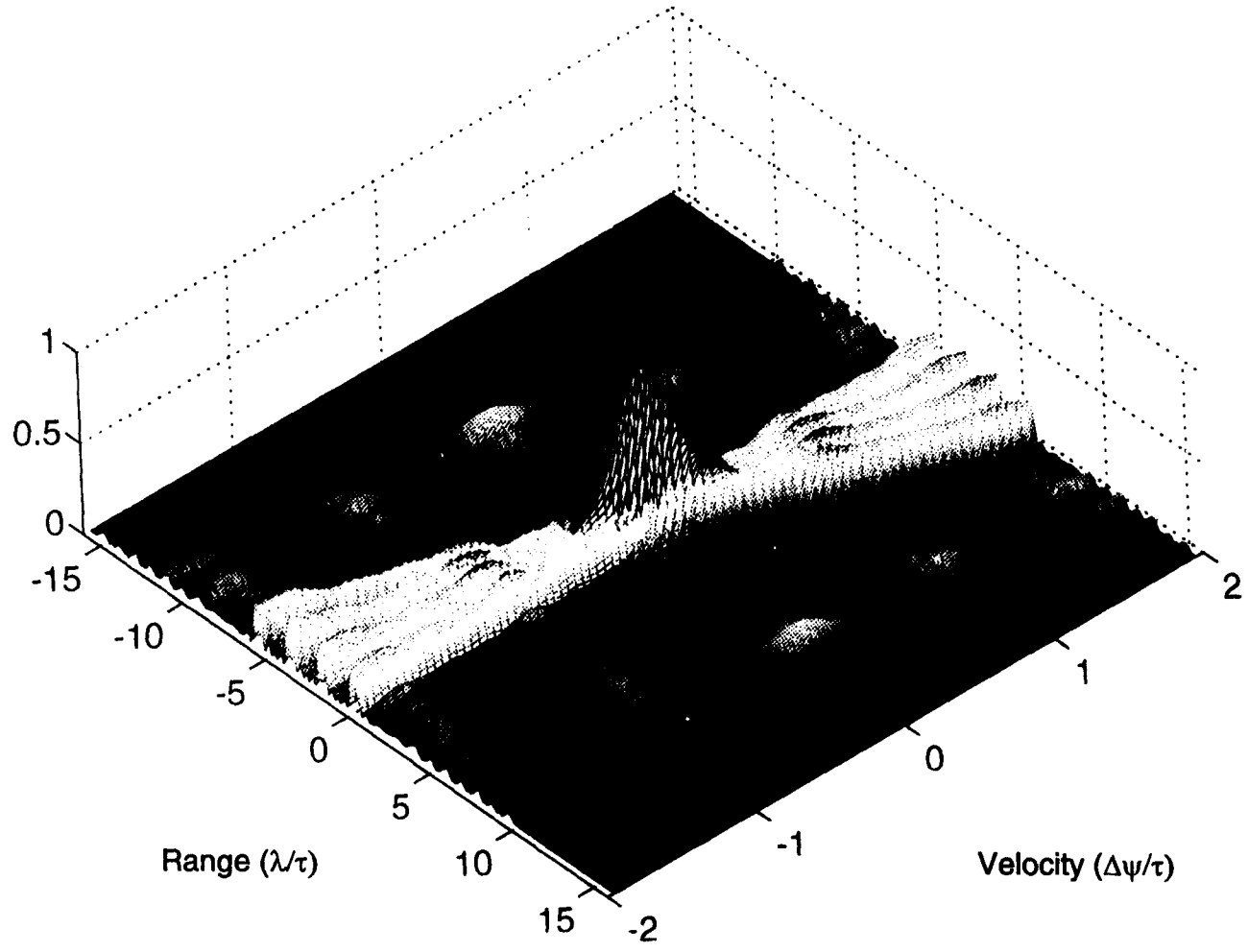

Figure 3.6. The Ambiguity Function of a Train of 4 UWB Radar Pulses.

Similarly, Figure 3.7 shows the same function in a contour presentation, where the symmetric property of the Ambiguity Function is evident.

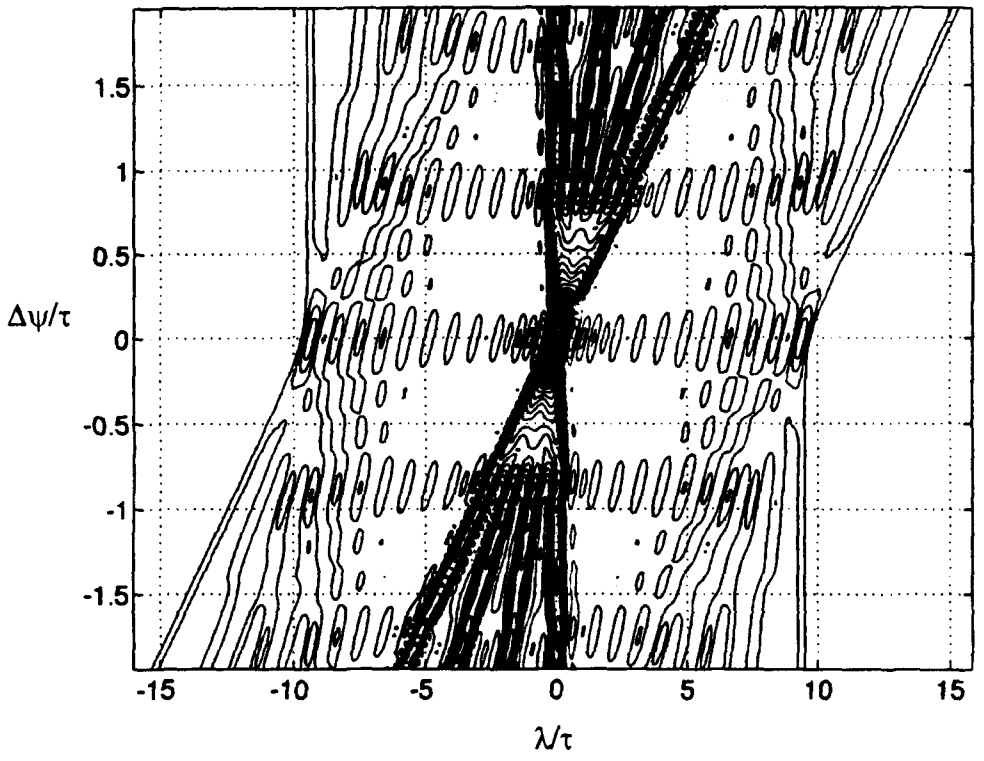

Figure 3.7. Contour Plot of the Ambiguity Function of 4 UWB Radar Pulses. Symmetry is clearly visible from this plot.

Figure 3.8 shows the change achieved by increasing the number of pulses from N = 4 to N = 16. Comparing Figure 3.8 with 3.6 it is noticeable that the Ambiguity Function approaches a thumbtack shape as the number of pulses increases.

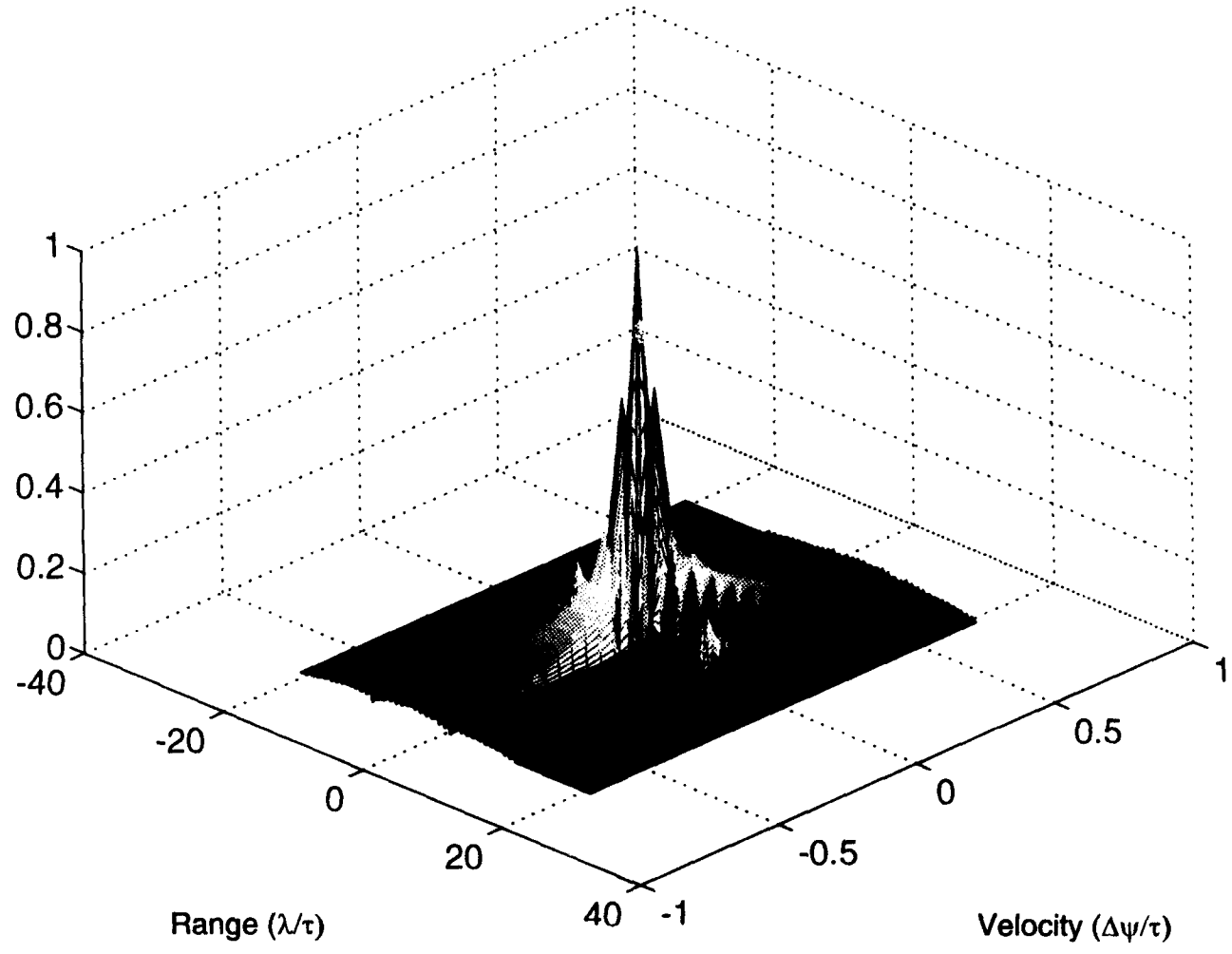

Figure 3.8. The Ambiguity Function of 16 UWB Radar Pulses. It clearly shows an approach to thumbtack Ambiguity Function.

4. Cuts Through the Ambiguity Function

The Ambiguity Function is a three-dimensional plot, which makes it hard to comprehend. A better insight can be obtained, however, by examining several one-dimensional cuts through the function. The most obvious is a cut along the time delay axis (λ/τ) which represents the correlation function of the signal at any particular doppler time difference $\Delta\psi$. Figure 3.9 shows some cuts of the Ambiguity Function of the Figure 3.6 for several values of $\Delta\psi$. From here it is evident that the amplitude of the signal increases as $\Delta\psi$ approaches zero. Similarly, Figure 3.10 shows some cuts of the Ambiguity Function of the Figure 3.8 ($N = 16$ pulses). Looking at both figures, it becomes evident than for $\Delta\psi \neq 0$, the amplitude of the signal decreases when N increases. In terms of a 3-D Ambiguity Function it means the peak to sidelobe ratio increases as number of pulses increases, which makes it possible to lower the detection threshold when larger numbers of pulses are used, resulting in an enhancement of detection performance.

5. Analysis of the Ambiguity Function Along the Velocity Axis $\Delta\psi/\tau$

An analysis of Figures 3.6 and 3.8 shows that a ridge is obtained along the velocity axis $\Delta\psi/\tau$ whose magnitude decreases as $1/N$ for $|\Delta\psi/\tau| > 0$. Figure 3.11 shows a view of the Ambiguity Function of Figure 3.6 ($N = 4$ pulses) along the velocity axis $\Delta\psi/\tau$.

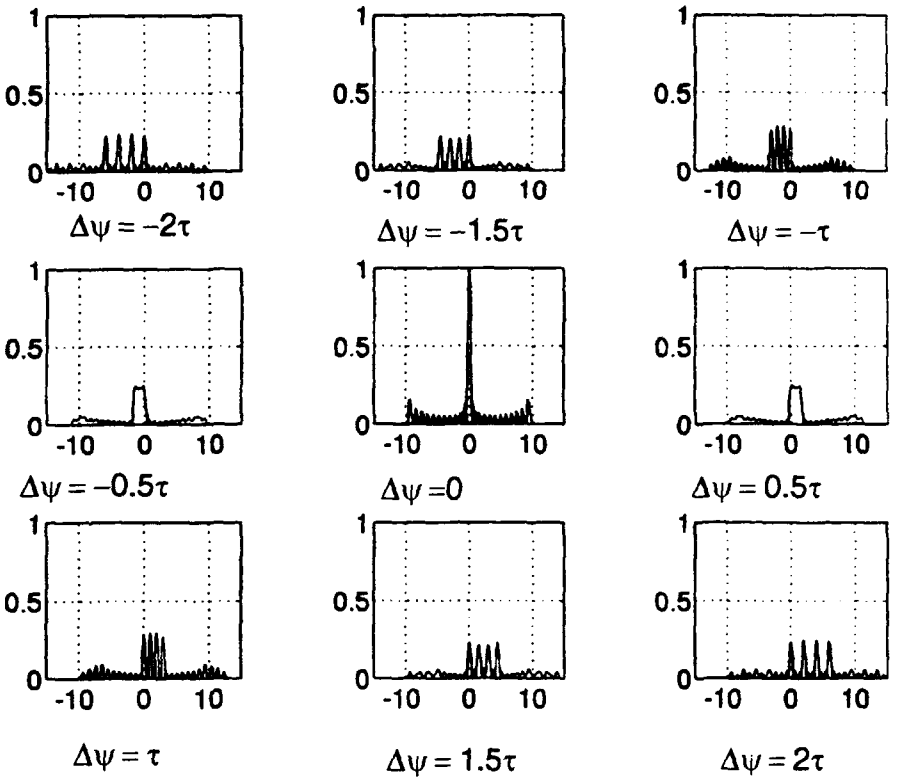

Figure 3.9. Cuts through the Ambiguity Function of Figure 3.6 for $\Delta\psi=\pm 2\tau$, $\pm 1.5\tau$, $\pm\tau$, $\pm 0.5\tau$, and 0.

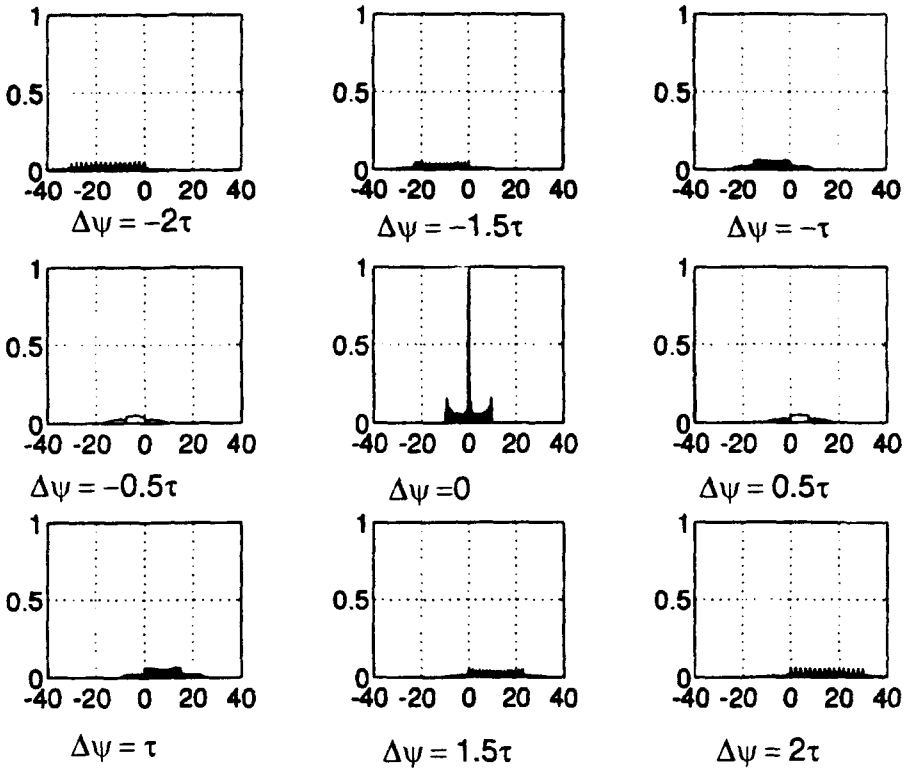

Figure 3.10. Cuts through the Ambiguity Function of Figure 3.8 for $\Delta\psi=\pm 2\tau$, $\pm 1.5\tau$, $\pm\tau$, $\pm 0.5\tau$, and 0.

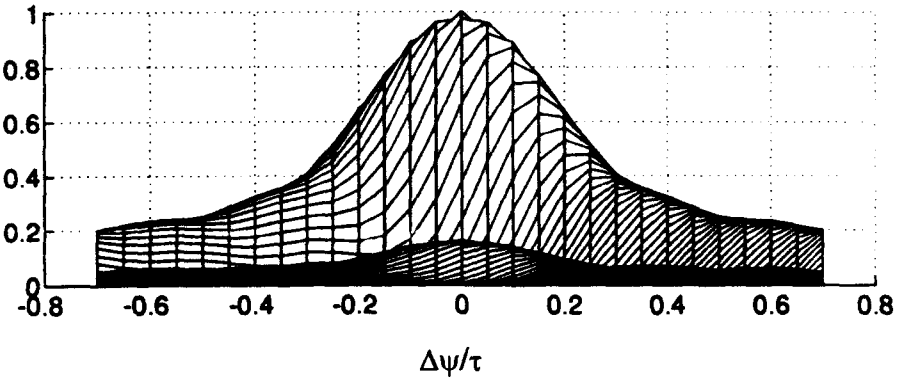

Figure 3.11. View of the Ambiguity Function of a Train of 4 UWB Radar Pulses along the Velocity Axis $\Delta\psi/\tau$ (Values Shown are from -0.7 to +0.7).

Figure 3.12 shows a view of the Ambiguity Function of Figure 3.9 (N = 16 pulses) along the velocity axis $\Delta\psi/\tau$. It can be seen that as the number of pulses increases so does the peak to sidelobe ratio.

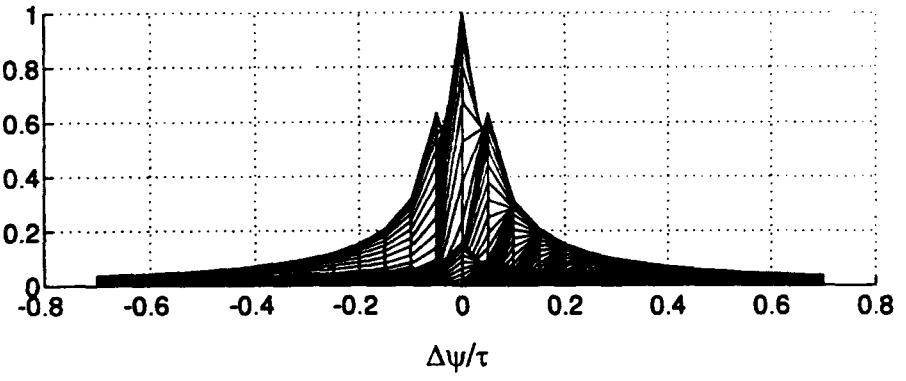

Figure 3.12. View of the Ambiguity Function of a Train of 16 UWB Radar Pulses along the Velocity Axis $\Delta\psi/\tau$.

The improvement achievable by increasing the number of pulses from N = 16 to N = 128 pulses is shown in Figure 3.13. From there it can be seen that the peak to sidelobe ratio increases dramatically as the number of pulses increases. This results in better velocity resolution, as seen below.

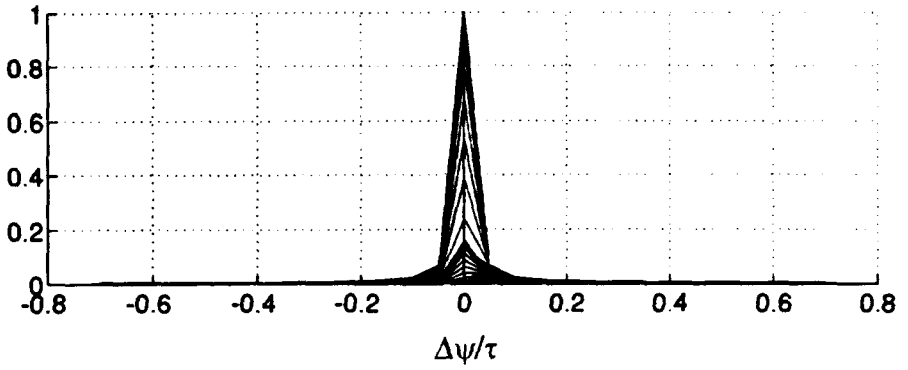

Figure 3.13. View of the Ambiguity Function of a Train of 128 UWB Radar Pulses along the Velocity Axis $\Delta\psi/\tau$.

The Ambiguity Function of Figure 3.13 for N = 128 pulses shows that a ridge is obtained along the velocity axis $\Delta\psi/\tau$ which stretches from -0.05 and +0. 05. As an example, using the waveform of Figure 3.2 with pulsewidth τ of 1 nsec and a repetition interval of 1 msec, the ridge on Figure 3.13 would corresponds to velocity resolution of

$$v = \frac{\Delta\psi}{2T}c = \frac{(\pm 0.05)(1\times 10^{-9})}{2(1\times 10^{-3})}(3\times 10^{8}) = \pm 7.5\frac{m}{sec}.$$

Furthermore, reducing the pulsewidth τ to 0.2 nsec and using the same repetition interval of 1 msec, the velocity resolution becomes

$$v = \frac{\Delta\psi}{2T}c = \frac{(\pm 0.05)(0.2\times 10^{-9})}{2(1\times 10^{-3})}(3\times 10^{8}) = \pm 1.5\frac{m}{sec}$$

This means that an enhancement of velocity resolution to ±1.5 msec could be achieved by reducing the pulsewidth τ from 1 to 0.2 nsec. As a consequence, the Ambiguity Function of Figure 3.13 for $N = 128$ allows the use of lower threshold, which would enhance target detection and keep false detections from the velocity sidelobes low.

B. AMBIGUITY FUNCTION OF A UWB PULSE TRAIN OF BARKER CODE OF LENGTH 13

Conventional and UWB radar waveform design techniques usually incorporate the pulse compression principle. Pulse compression is a technique that obtains high range resolution using coded signals of longer duration. Coding of UWB radar pulses can be accomplished using phase-coding sequences, such as Barker codes and complementary codes. Barker codes have the advantage that their sidelobe structures contain the minimum energy theoretically possible. The disadvantage is that the largest value is equal to 13, which limits the pulse compression ratio.

1. Transmitted UWB Waveform

Figure 3.14 shows a radiated waveform consisting of a train of four UWB radar pulses. The pulses are coded with Barker code of length 13 and generated by using the FSM with sixty-five sources. Every pulse has a width τ and repetition interval T.

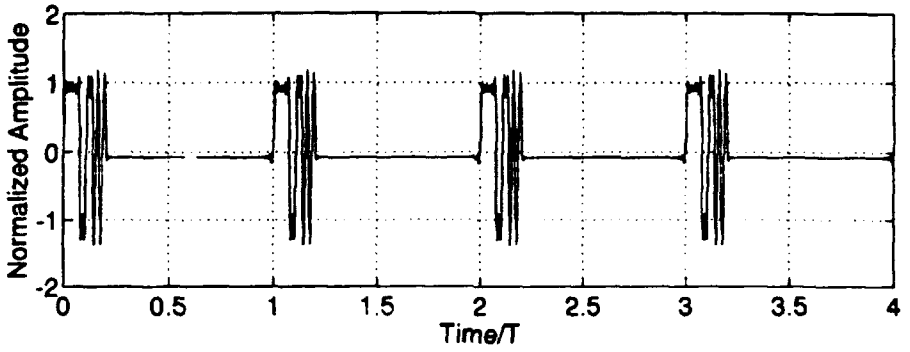

Figure 3.14. Train of 4 UWB Radar Pulses Coded with Barker Length 13 Generated using the FSM with 65 Oscillators.

2. Processing of the Received UWB Signal

A computer simulation of the block diagram of Figure 3.1 is used to obtain outputs of the UWB radar processor. Figure 3.15 shows the output of the matched filter using the waveform of Figure 3.14 as input.

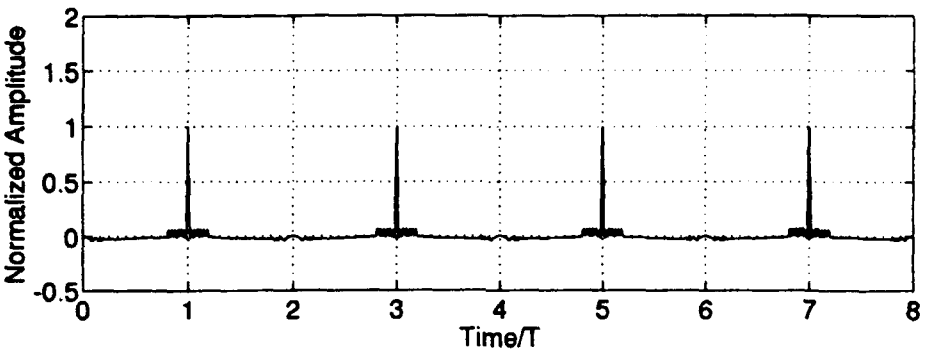

Figure 3.15. Normalized Output of Matched Filter for 4 UWB Radar Pulses Coded with Barker Length 13.

After the matched filtering process has been performed, the signal is passed through a bank of doppler processors. As it was established earlier, the output of the doppler processor is a function of the doppler time difference $\Delta\psi$. Figure 3.16 shows the output of doppler processor bank for various values of doppler time difference $\Delta\psi$ using four pulses as input (N = 4).

From this figure it can be seen that the peak amplitude of the output signal is a function of $\Delta\psi$. As $\Delta\psi$ approach zero, the peak amplitude increases and the duration of the signal decreases.

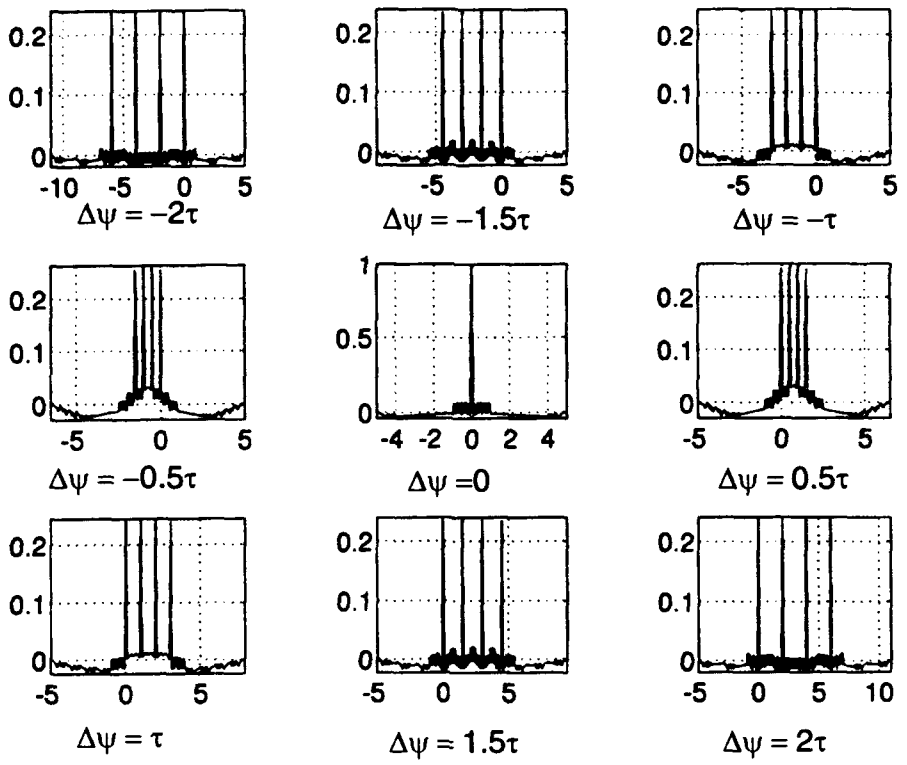

Figure 3.16. Doppler Processor Bank Output for N=4 Barker 13 Pulses.

Computer simulation also shows that for the same doppler time difference $\Delta\psi$, an increasing number of pulses reduces the amplitude of the doppler processor output for $\Delta\psi \neq 0$. Figure 3.17 shows the output of the Doppler processor bank using sixteen pulses as input (N = 16). Comparing Figures 3.16 and 3.17 it is evident that as N increases, doppler processor output amplitudes for $\Delta\psi \neq 0$ are reduced.

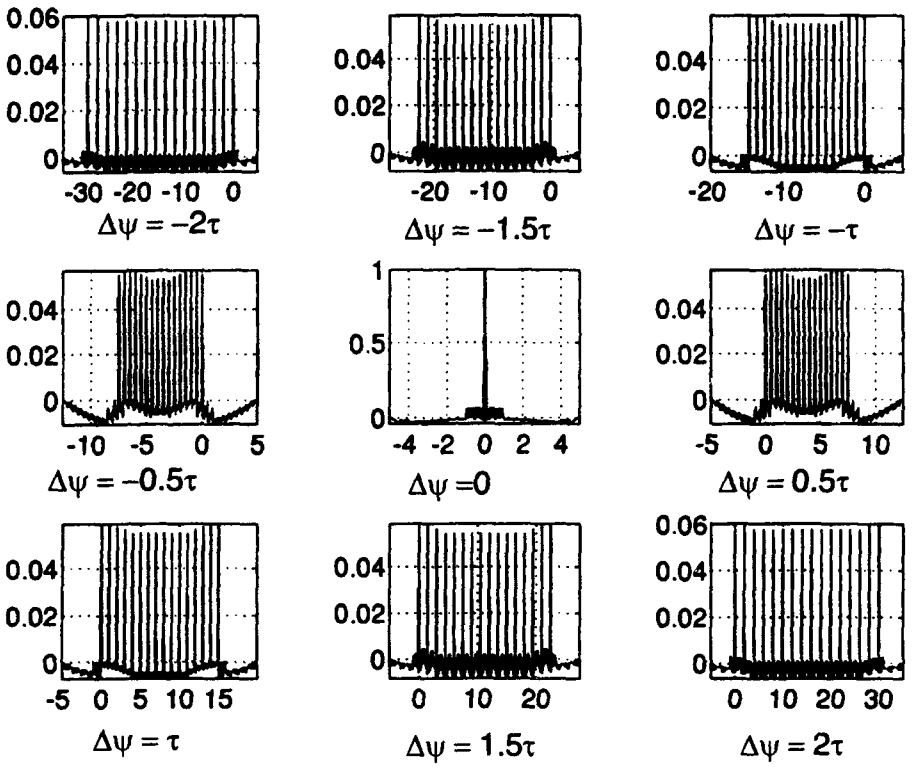

Figure 3.17. Doppler Processor Bank Output for N=16 Barker 13 Pulses.

3. Ambiguity Function

A computer simulation of the block diagram of Figure 3.1 is used to compute the Ambiguity Function defined by Equation (2.36). The Ambiguity Function for a train of UWB radar pulses coded with Barker length 13 when **N = 4** is shown in Figure 3.18. Similarly Figure 3.19 shows the same function in a contour presentation where the symmetry property of the Ambiguity Function can be noted. Figure 3.20 shows the change achieved in the shape of the Ambiguity Function by increasing the number of pulses from **N=4** to **N=16**. Comparing Figure 3.18 and 3.20 it can be concluded that the Ambiguity Function approaches a thumbtack shape as the number of pulses increases.

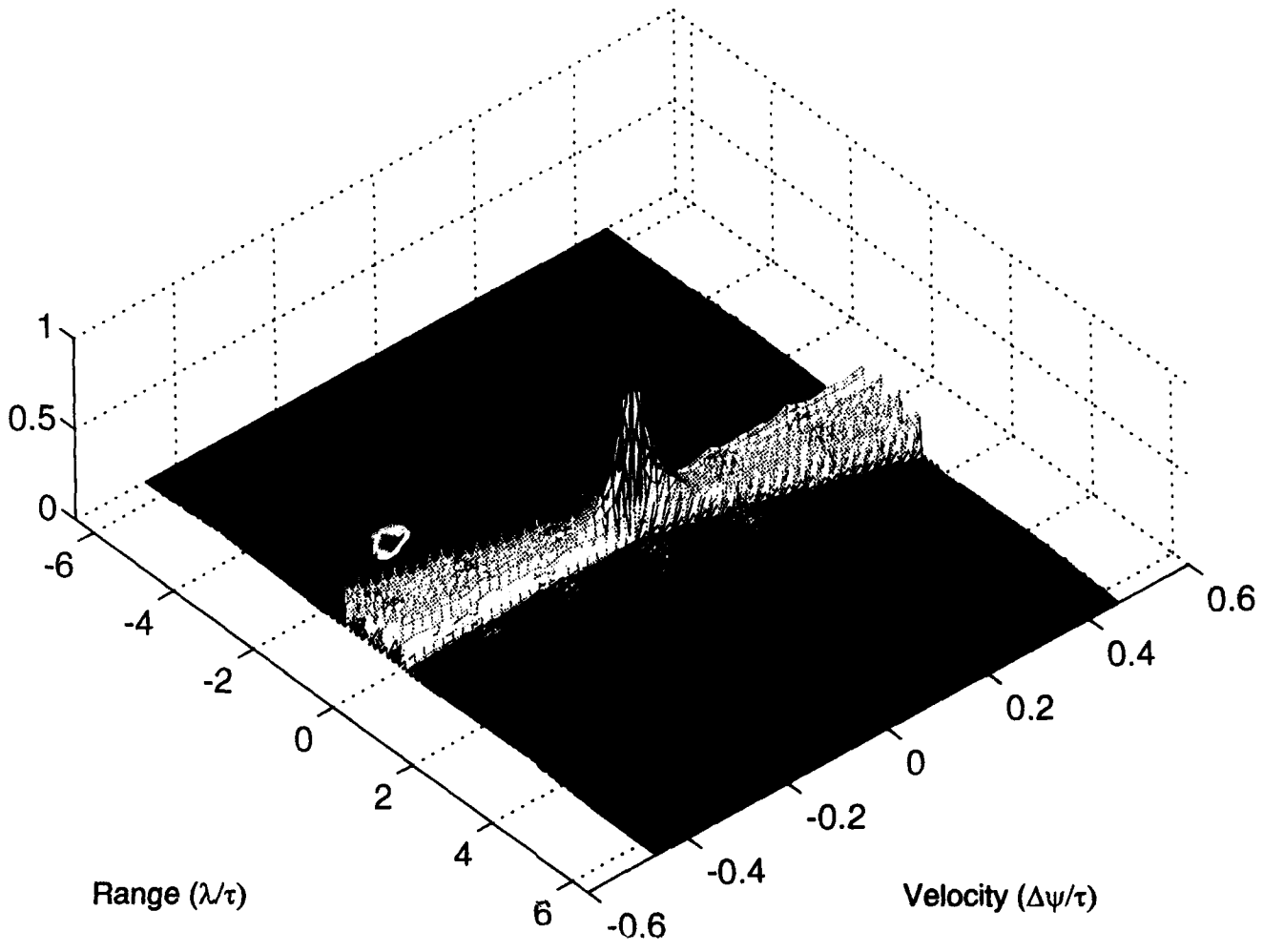

Figure 3.18. The Ambiguity Funcion of a Train of 4 UWB Barker 13 Pulses.

4. Cuts Through the Ambiguity Function

Some insight into three-dimensional plots of the Ambiguity Function can be obtained by looking at several one-dimensional cuts through the function. The most obvious is a cut along the time delay axis (λ/τ) which represents the correlation function of the signal at any particular doppler time difference $\Delta\psi$. Figure 3.21 shows some cuts of the Ambiguity Function of the Figure 3.18 for several values of $\Delta\psi$. From this it is evident that the amplitude of the signal increases as $\Delta\psi$ approaches zero.

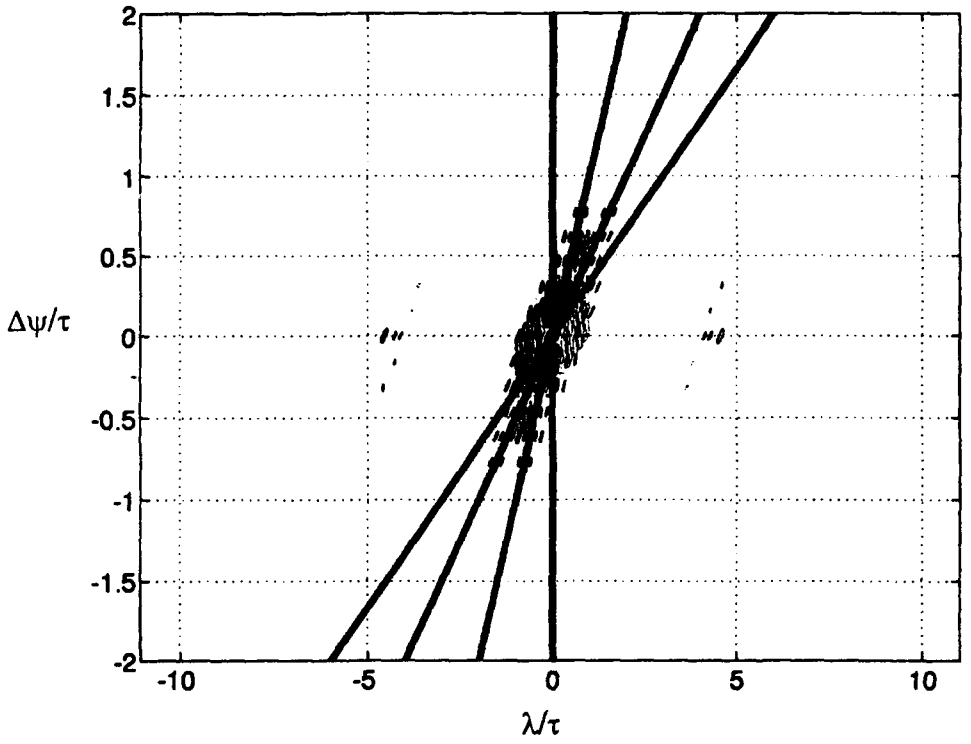

Figure 3.19. Contour Plot of the Ambiguity Function of 4 UWB Barker 13 Radar Pulses. Symmetry is clearly visible from this plot.

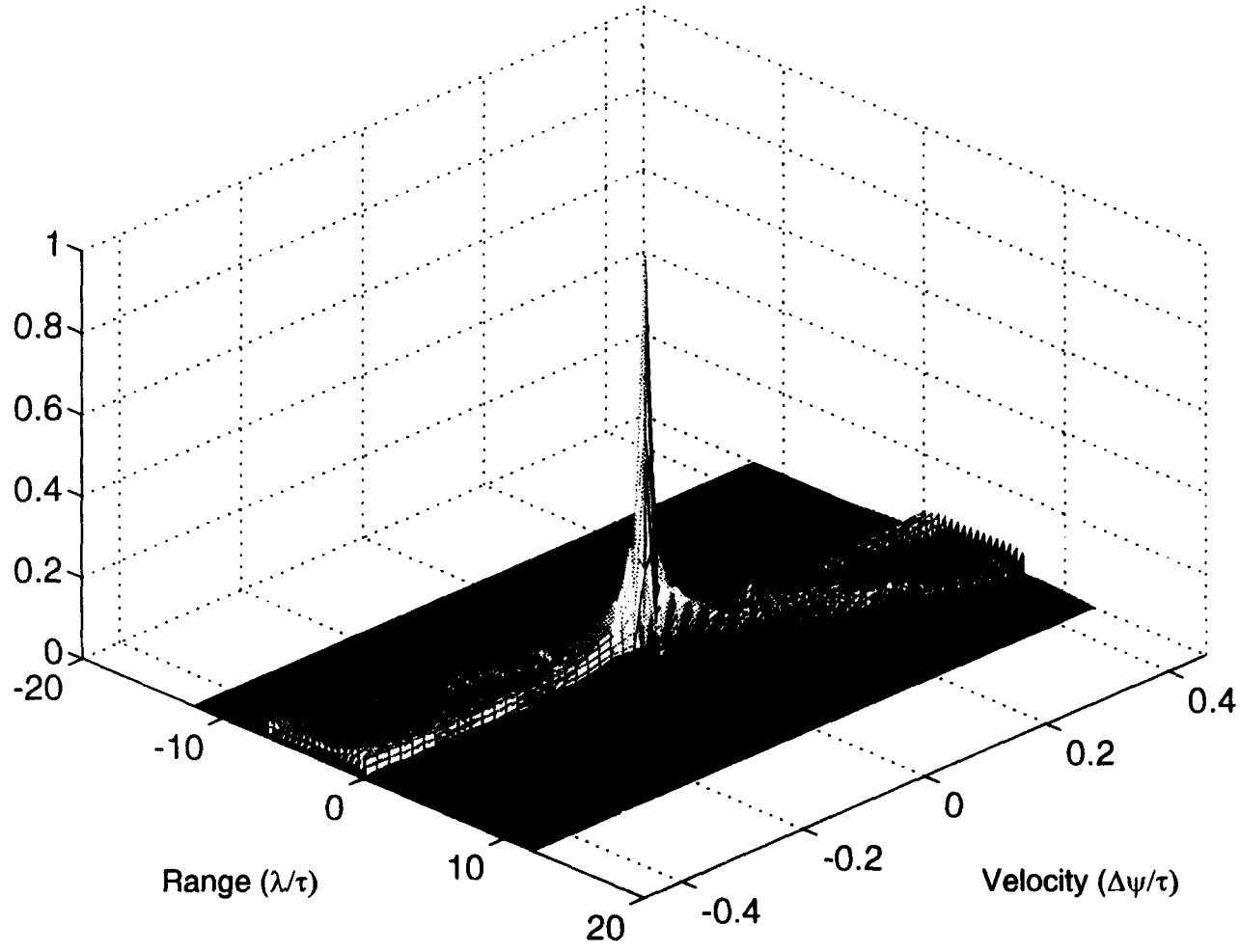

Figure 3.20. The Ambiguity Function of 16 UWB Barker 13 Radar Pulses. It clearly shows an approach to thumbtack Ambiguity Function.

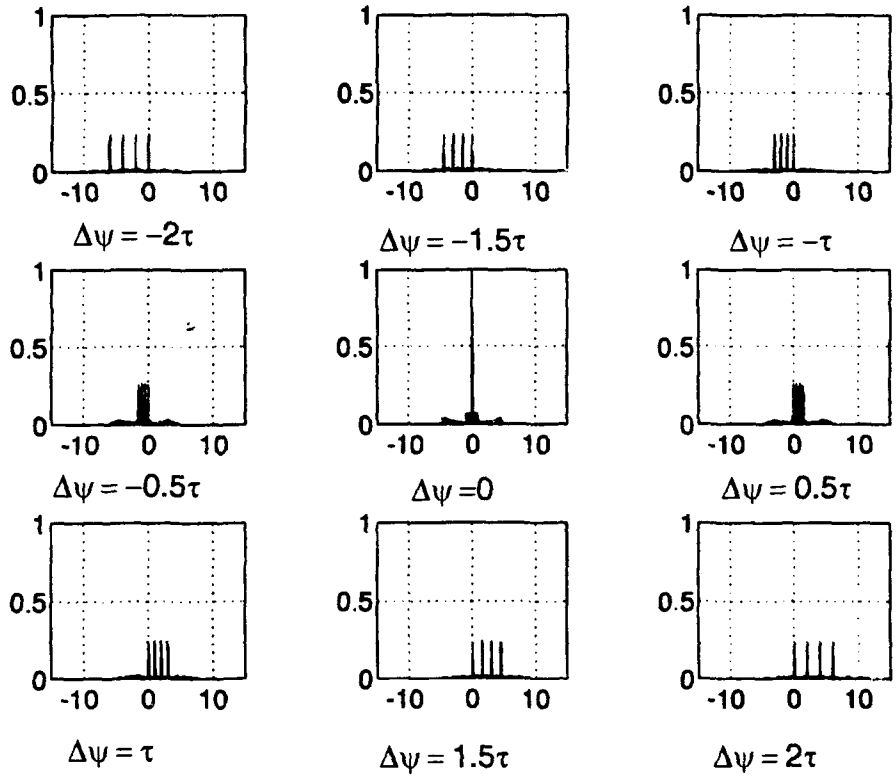

Figure 3.21. Cuts through the Ambiguity Function of Figure 3.18 for $\Delta\psi=\pm 2\tau$, $\pm 1.5\tau$, $\pm\tau$, $\pm 0.5\tau$, and 0.

Similarly, Figure 3.22 shows some cuts of the Ambiguity Function of the Figure 3.20 (N = 16 pulses).

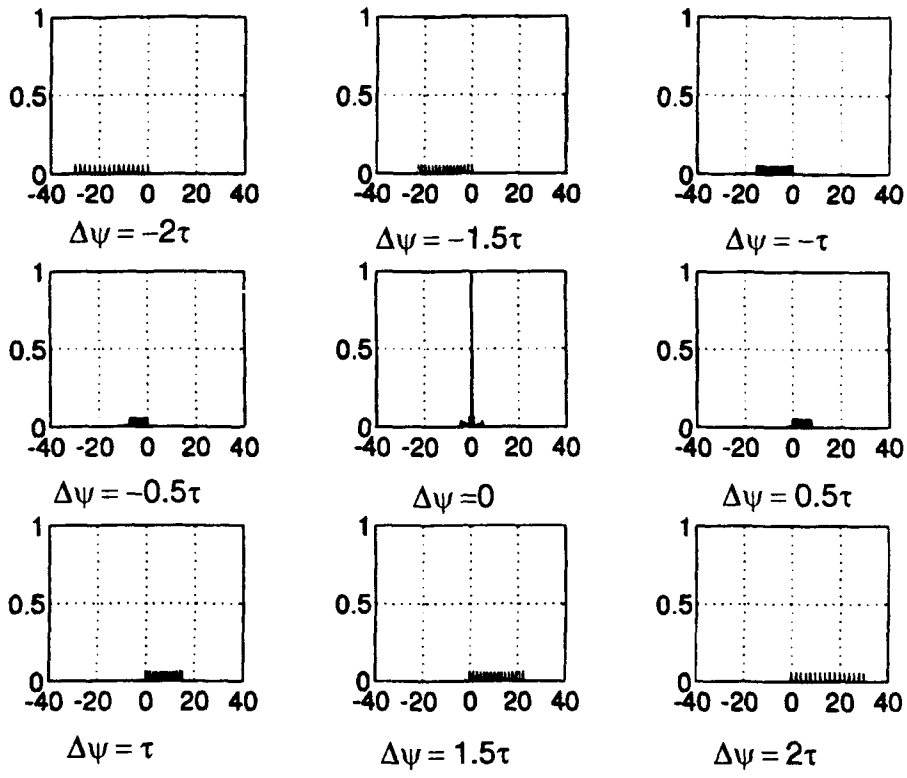

Figure 3.22. Cuts through the Ambiguity Function of Figure 3.20 for $\Delta\psi=\pm 2\tau$, $\pm 1.5\tau$, $\pm\tau$, $\pm 0.5\tau$, and 0.

From both figures it becomes evident than for $\Delta\psi \neq 0$, the amplitude of the signal decreases when N increases. In terms of a 3-D Ambiguity Function, the peak to sidelobe ratio increases as number of pulses increases. This makes it possible to lower detection threshold when larger numbers of pulses are used, which results in an enhancement of the detection performance.

5. Analysis of the Ambiguity Function Along the Velocity Axis $\Delta\psi/\tau$

An analysis of Figures 3.18 and 3.20 shows that a ridge is obtained along the velocity axis $\Delta\psi/\tau$. The magnitude decreases by 1/N for $|\Delta\psi/\tau| > 0$. Figure 3.23 shows a view of the Ambiguity Function of Figure 3.18 (N = 4 pulses) along the velocity axis $\Delta\psi/\tau$.

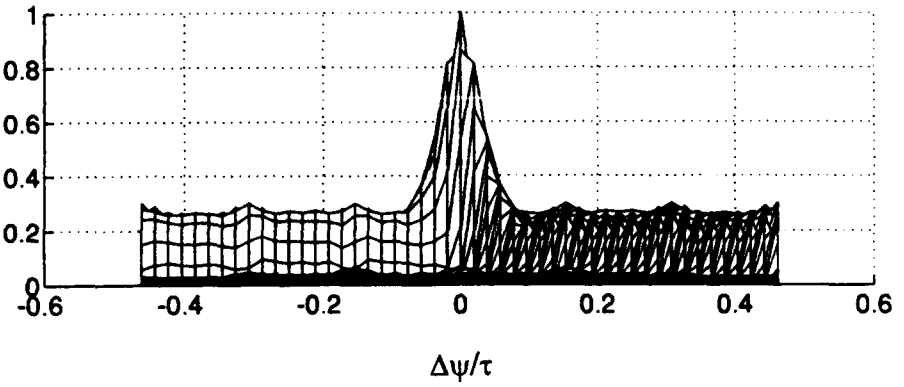

Figure 3.23. View of the Ambiguity Function of a Train of 4 UWB Barker 13 Radar Pulses along the Velocity Axis $\Delta\psi/\tau$ (Values Shown are from -0.46 to +0.46).

Figure 3.24 shows a view of the Ambiguity Function of Figure 3.20 (N = 16 pulses) along the velocity axis $\Delta\psi/\tau$. It can be seen that as the number of pulses increases, so does the peak-to-sidelobe ratio.

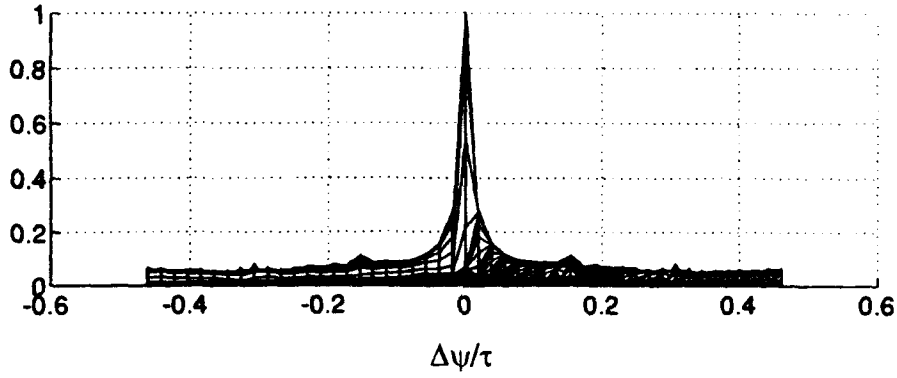

Figure 3.24. View of the Ambiguity Function of a Train of 16 UWB Barker 13 Radar Pulses along the Velocity Axis $\Delta\psi/\tau$.

The improvement achievable by increasing the number of pulses from N = 16 to N = 128 is shown in Figure 3.25. It can be seen that the peak to sidelobe ratio increases dramatically as the number of pulses increases, resulting in a better velocity resolution, as seen below.

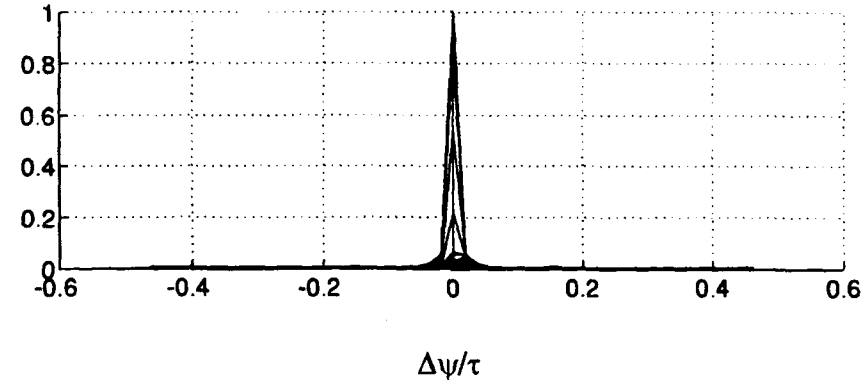

Figure 3.25. View of the Ambiguity Function of a Train of 128 UWB Barker 13 Radar Pulses along the Velocity Axis $\Delta\psi/\tau$.

The Ambiguity Function of Figure 3.25 for N = 128 pulses shows that a ridge is obtained along the velocity axis $\Delta\psi/\tau$ which stretches from -0.02 and +0.02. As an example, using the waveform of Figure 3.14 with pulsewidth τ of 1 nsec and a repetition interval of 1 msec, the ridge on Figure 3.25 would corresponds to velocity resolution of

$$v = \frac{\Delta\psi}{2T}c = \frac{(\pm 0.02)(1 \times 10^{-9})}{2(1 \times 10^{-3})}(3 \times 10^{8}) = \pm 3.15 \frac{m}{sec}$$

Furthermore, considering the same pulse repetition interval of 1 msec, a reduction to the pulsewidth τ from 1 nsec to 0.2 nsec would change the velocity resolution to

$$v = \frac{\Delta\psi}{2T}c = \frac{(\pm 0.02)(0.2 \times 10^{-9})}{2(1 \times 10^{-3})}(3 \times 10^{8}) = \pm 0.6 \frac{m}{sec}$$

which means that an enhancement of velocity resolution to ± 0.6 m/sec could be achieved by reducing the pulsewidth τ to 0.2 nsec, which represents, in terms of radar, a very good velocity resolution. As a consequence, the Ambiguity Function of Figure 3.25 forN=128 allows the use of a lower threshold, enhancing target detection and keeping false detections from the velocity sidelobes low.

IV. CONCLUSIONS AND RECOMMENDATIONS

A. CONCLUSIONS

This thesis has generated the Ambiguity Function for two different UWB radar waveforms produced by the Fourier Synthesis Method. This waveform generation method consists of combining a large number of continuous-wave oscillators operating at harmonically related frequencies in order to create a coherent train of pulses. This approach offers a major advantage over other methods in that very short pulses can be produced in a coherent and controllable form, and high average power can be generated at lower switching speeds and with lower power sources.

The Ambiguity Functions of the UWB radar waveforms generated in this thesis move very quickly toward a thumbtack shape when the number of pulses of the received signal increase, which means that velocity resolution can be improved by increasing the duration of the UWB radar signal received from a target. Similarly, the peak-to-sidelobe ratio of the Ambiguity Function increases along with the number of pulses. This makes it possible to lower the detection threshold when a larger number of pulses are used, resulting in an enhancement of the detection process.

This thesis has also shown that the Ambiguity Function of a UWB radar waveform can be improved by coding. In fact, the thumbtack Ambiguity Function of the UWB

waveform coded with Barker code of length 13 can easily be achieved by increasing the processed number of pulses, which makes it simpler to obtain nigher velocity resolution.

Finally, the results obtained in this thesis show that UWB radar waveforms are capable of achieving resolutions that are difficult to obtain with conventional radars. For such resolutions, conventional radars require operation at appreciably higher frequencies, which results in additional signal attenuation and, consequently, lower overall radar ranges. Thus, one of the major advantages of using UWB radar waveforms is their ability to achieve much better resolution at lower frequencies. This advantage is very significant for applications requiring foliage or ground penetration, where the use of low frequencies has enabled levels of detection which are considered difficult for conventional radar waveforms.

B. RECOMMENDATIONS

One area for further research involves generation of Ambiguity Functions considering other UWB radar waveforms produced by the Fourier Synthesis Method. These include linear frequency modulated (chirp) signals and UWB radar waveforms generated with complex coding techniques, such as complementary code pairs, polyphase codes or Costas sequence codes.

APPENDIX A. THE FOURIER SYNTHESIS METHOD

Fourier Series allow the representation of a periodic waveform $x(t)$ as the sum of sinusoids whose frequencies are multiples of the fundamental frequency. The radar signal can be approximated as

$$x(t) = \sum_{n=1}^{N} (a_n \cos n\omega_0 t + b_n \sin n\omega_0 t)$$

where $\omega_0 = 2\pi f$; $f = 1/T$, T is the period of the function and the coefficients a_n and b_n represent the unknown amplitudes of the cosine and sine terms. Since the DC term cannot be radiated, it is held to be zero in the expression.

Fourier Series make it possible to generate a periodic train of pulses by a summation of all the frequency spectral components of the pulse train. Applying this important concept to a radar system, it becomes possible to generate a periodic train of pulses by using a transmitting source for each spectral component and coherently radiating these signals through an antenna. This radar waveform generation method is known as the Fourier Synthesis Method (FSM), and offers several advantages when used in UWB radar systems. For instance, very short pulses can be generated in a coherent and controllable form and lower switching speeds and lower power sources can be used. Additionally, the FSM can mitigate the high peak power problem often encountered in UWB radar waveforms.

Figure A.1 shows a schematic diagram of a UWB radar transmitter based on the FSM concept. During transmission, each frequency source is tuned to one of the spectral frequencies needed to form the required train of pulses. A common master oscillator is used to achieve phase coherency in all frequency sources. A coherent summation of all frequency source outputs is performed in a multiplexer, forming the required UWB radar waveform, which is transmitted through the antenna. Depending on the required radar application, the duration of the transmitted waveform may be controlled by on-off switches.

A more comprehensive treatment of the FSM can be found in "Waveform Generation for Ultra Wideband Radar Systems", a Naval Postgraduate School Master's Thesis written by H.F. Chiang and presented in December, 1993.

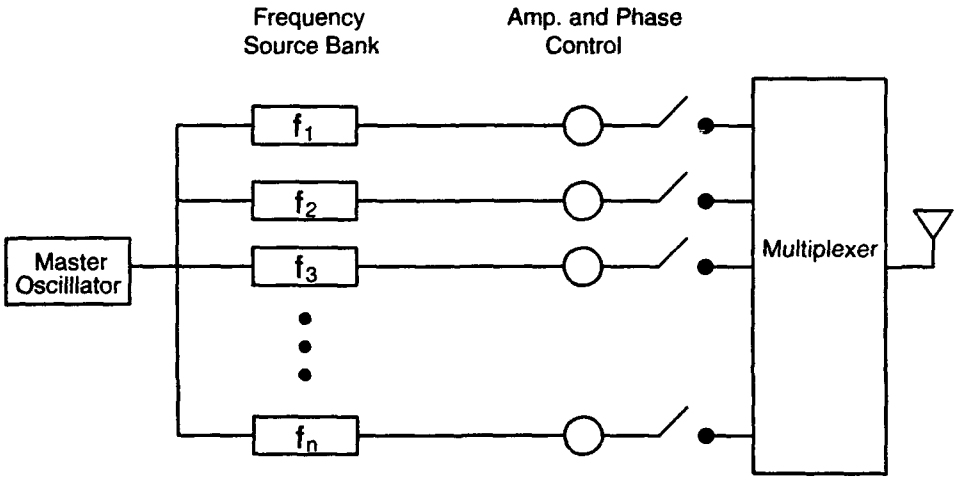

Figure A.1. Diagram of a UWB Radar Transmitter based on the FSM [Ref. 16].

APPENDIX B. PROGRAM CODES

This appendix contains the high level source code used in development of the ambiguity function simulation in Chapters II and III. The source code is in MATLAB which is a "C-Based" development language. MATLAB is defined as an interactive system whose basic data element is a matrix and is especially design to solve numerical problems in a fraction of time it would take to write program in a language such as Fortran, Basic or C [Ref. 17].

```
% PROGRAM TITLE: rect.m

% THIS PROGRAM CALCULATE THE AMBIGUITY FUNCTION FOR
% A UWB RADAR IDEAL RECTANGULAR SIGNAL

%lambda    = time delay
%N         = number of transmitted pulses
%Tb        = time base (unit of time)
%T         = pulse repetition interval
%tau       = pulse width
%phi       = doppler time of the signal
%phiz      = doppler time of the processor
%delta(phi) = doppler time difference

clear
clc
clg
Tb=100;
tau=0.2*Tb;
N=input('Enter number of transmitted pulses: ')
for M=1:81
        outrect=frect(N,M);
        t=1:length(outrect);
        outptrec(M,t)=outrect;
end
outptrec=abs(outptrec);
n=num2str(N);
mesh(-((length(outptrec)/2)+1)/tau:1/tau:...     %PLOT AMB.FUNCTION
((length(outptrec)/2)-2)/tau,...
-40/tau:1/tau:40/tau, outptrec )
```

```
grid
view(40,30);
xlabel('lambda/tau')
ylabel('DELTA(phi)/tau')
title(['AMBIGUITY FUNCTION OF IDEAL RECTANGULAR SIGNAL FOR N = ',n,''])
print rect1
pause
contour(-((length(outptrec)/2)+1)/tau:1/tau:...  %CONTOUR AMB.FUNCTION
((length(outptrec)/2)-2)/tau,...
-40/tau:1/tau:40/tau, outptrec )
grid
xlabel('lambda/tau')
ylabel('DELTA(phi)/tau')
title(['CONTOUR PLOTS IDEAL RECTANGULAR SIGNAL AMBIGUITY FUNCTION N = ',n,''])
print rect2



function y=frect(N,M)

% THIS FUNCTION PRODUCES RECTANGULAR PULSES AND ALLOWS
% CORRELATES THEM AND TO PRODUCE OUTPUT FOR THE DOPPLER
% PROCESSOR.

%*************************************************************
%       THIS PROGRAM PRODUCES A SINGLE RECTANGULAR PULSE
%*************************************************************

Tb=100;
T=2*Tb;
tau=0.2*Tb;
phi=41;
z=zeros(1,2*Tb);
o=ones(1,0.2*Tb);
sr=[o];
srt=[o zeros(1,T-tau)];
tr=0:T-1;
tr=tr/T;
subplot(2,1,1),
plot(tr,srt)                    %PLOT RECTANGULAR PULSE
grid
xlabel('Time/T')
ylabel('Normalized Amplitude')
title('UWB IDEAL RECTANGULAR PULSE')

%*************************************************************
%       THIS PROGRAM PRODUCES TRAIN OF N RECTANGULAR PULSES
%*************************************************************

srN=[];
for n=1:N
```

```
        srN=[srN srt];
end
trN=[1:length(srN)];
trN=trN/T;
subplot(2,1,2),
plot(trN,srN)                          %PLOT TRAIN RECT.PULSES
grid
xlabel('Time/T')
ylabel('Normalized Amplitude')
title('TRAIN OF UWB IDEAL RECTANGULAR PULSES')
print frect1
pause

%************************************************************************
%   THIS PROGRAM PRODUCES AUTOCORRELATION OF SINGLE RECTANGULAR PULSE
%************************************************************************

slidout=xcorr(sr);
slidout=slidout';
slidout=slidout/max(slidout);
ts=0:length(slidout)-1;
ts=ts/T;
subplot(2,1,1),
plot(ts,slidout)              %PLOT AUTOCORRELATION RECT.PULSE
grid
xlabel('Time/T')
ylabel('Normalized Amplitude')
title('MATCHED FILTER OUTPUT OF UWB IDEAL RECTANGULAR PULSE')

%************************************************************************
% THIS PROGRAM PRODUCES AUTOCORRELATION OF TRAIN OF N RECTANGULAR
PULSES
%************************************************************************

corrout=[];
for n=1:N
        corrout=[corrout slidoutN];
end

tc=[1:length(corrout)];
tc=tc/T;
subplot(2,1,2),
plot(tc,corrout)              %PLOT AUTOCORRELATION TRAIN RECT.PULSES
grid
xlabel('Time/T')
ylabel('Normalized Amplitude')
title('MATCHED FILTER OUTPUT FOR TRAIN UWB IDEAL RECTANGULAR PULSES')
print frect2
pause


%****************************************************************
```

```
% THIS PROGRAM PRODUCES OUTPUT OF DOPPLER PROCESSOR
%*****************************************************************

Doplrout=slidout;
input=slidout;
phiz=M;
for n=1:N-1
        input=[zeros(1,(phi)) input];
        feedout=[zeros(1,(phiz)) Doplrout];

        if phiz >= phi
                Doplrout=feedout+[input zeros(1,n*(phiz-phi))];


        else
                Doplrout=input+[feedout zeros(1,(phi-phiz))];
        end

end

procorout=Doplrout/N;
t=0:length(procorout)-1;
t=t/tau;
plot(t,procorout)               %PLOT DOPPLER PROCESSOR OUTPUT
grid
xlabel('lambda/tau')
ylabel('Normalized Amplitude')
delta(phi)=num2str((phiz-phi)/tau)
gtext(['(delta(phi)) = ',delta(phi),'tau FOR RECTANGULAR PULSE SIGNAL (N=4)'])
print frect3

y=procorout;


% PROGRAM TITLE: uncod.m

% THIS PROGRAM CALCULATES THE AMBIGUITY
% FUNCTION FOR A UWB RADAR SIGNAL

%lambda    = time delay
%h         = number of harmonics
%N         = number of transmitted pulses
%Tb        = time base (unit of time)
%T         = pulse repetition interval
%tau       = pulse width
%phi       = doppler time of the signal
%phiz      = doppler time of the processor
%delta(phi) = doppler time difference

clear
clc
clg
```

```
Tb=100;
tau=0.2*Tb;
N=input('Enter number of transmitted pulses:  ')
for M=1:81
        outsinc=funcod(N,M);
        t=1:length(outsinc);
        outpsinc(M,t)=outsinc;
end
outpsinc=abs(outpsinc);
n=num2str(N);
mesh(-((length(outpsinc)/2)+1)/tau:1/tau:...    %PLOT AMB.FUNCTION
((length(outpsinc)/2)-2)/tau,...
-40/tau:1/tau:40/tau, outpsinc )
grid
view(50,60);
xlabel('lambda/tau')
ylabel('DELTA(phi)/tau')
title(['AMBIGUITY FUNCTION OF UWB RADAR SIGNAL FOR N = ',n,''])
print uncod1
pause
contour(-((length(outpsinc)/2)+1)/tau:1/tau:... %CONTOUR AMB.FUNCTION
((length(outpsinc)/2)-2)/tau,...
-40/tau:1/tau:40/tau, outpsinc )
grid
xlabel('lambda/tau')
ylabel('DELTA(phi)/tau')
title(['CONTOUR PLOTS OF UWB RADAR SIGNAL AMBIGUITY FUNCTION FOR N = ',n,''])
print uncod2



function y=funcod(N,M)

% THIS FUNCTION PRODUCES UWB RADAR PULSES AND ALLOWS
% CORRELATES THEM AND TO PRODUCE OUTPUT FOR THE DOPPLER
% PROCESSOR.

%************************************************************
%       THIS PROGRAM PRODUCES A SINGLE UWB UNCODED PULSE
%************************************************************

h=11;
Tb=100;
T=2*Tb;
t=-0.1:1/Tb:1.9;
tau=0.2*Tb
phi=41;
fo=0.5;
wo=2*pi*fo;
A=1;
bn=0;
for i=1:1:h
```

```
        bi=cos(i*wo*t);
        bn=bn+bi;
end
bn=bn/h;
subplot(2,1,1),
plot(t,bn)                          %PLOT UWB RADAR PULSE
grid
xlabel('Time/T')
ylabel('Normalized Amplitude')
title('UWB RADAR PULSE')

%*************************************************************
%       THIS PROGRAM PRODUCES TRAIN OF N UWB RADAR PULSES
%*************************************************************

srN=[];
for n=1:N
        srN=[srN bn];
end
trN=0:length(srN)-1;
trN=trN/T;
subplot(2,1,2),
plot(trN,srN)                       %PLOT N UWB RADAR PULSES
grid
xlabel('Time/T')
ylabel('Normalized Amplitude')
title('TRAIN OF UWB RADAR PULSES')
print funcod1
pause

%*************************************************************
%   THIS PROGRAM PRODUCES AUTOCORRELATION OF SINGLE UWB PULSE
%*************************************************************

slidout=xcorr(bn);
slidout=slidout';
slidout=slidout/max(slidout) ;
ts=0:length(slidout)-1;
ts=ts/T;
subplot(2,1,1),
plot(ts,slidout)            %PLOT AUTOCORRELATION UWB RADAR PULSE
grid
xlabel('Time/T')
ylabel('Normalized Amplitude')
title('MATCHED FILTER OUTPUT OF UWB RADAR PULSE')

%*************************************************************
% THIS PROGRAM PRODUCES AUTOCORRELATION OF TRAIN OF N UWB PULSES
%*************************************************************

corrout=[];
for n=1:N
```

```
        corrout=[corrout slidout];
end

tc=0:length(corrout)-1;
tc=tc/T;
subplot(2,1,2),
plot(tc,corrout)        %PLOT AUTOCORRELATION N UWB RADAR PULSES
grid
xlabel('Time/T')
ylabel('Normalized Amplitude')
title('MATCHED FILTER OUTPUT FOR TRAIN OF UWB RADAR PULSES')
print funcod2
pause

%*****************************************************************
% THIS PROGRAM PRODUCES OUTPUT OF DOPPLER PROCESSOR
%*****************************************************************

Doplrout=slidout;
input=slidout;
phiz=M;
for i=1:N-1
        input=[zeros(1,(phi)) input];
        feedout=[zeros(1,(phiz)) Doplrout];

        if phiz >= phi
                Doplrout=feedout+[input zeros(1,i*(phiz-phi))];
        else
                Doplrout=input+[feedout zeros(1,(phi-phiz))];
        end

end

procorout=Doplrout/N;
tp=[0:length(procorout)-1];
tp=tp/tau;
plot(tp,procorout)                      %PLOT DOPPLER PROCESSOR OUTPUT
grid
xlabel('lambda/tau')
ylabel('Normalized Amplitude')
delta(phi)=num2str((phiz-phi)/tau)
gtext(['(delta(phi)) = ',delta(phi),'tau FOR UWB RADAR SIGNAL (N=4)'])
print funcod3
pause

y=procorout;
```

```
% PROGRAM TITLE: bark13.m

% THIS PROGRAM CALCULATE THE AMBIGUITY
% FUNCTION FOR A UWB RADAR SIGNAL CODED
% UNDER BARKER CODE 13

%lambda    = time delay
%h         = number of harmonics
%N         = number of transmitted pulses
%Tb        = time base (unit of time)
%T         = pulse repetition interval
%tau       = pulsewidth
%phi       = doppler time of the signal
%phiz      = doppler time of the processor
%delta(phi) = doppler time difference

clear
clc
clg
Tb=65;
T=4*Tb;
tau=13*T/Tb;
N=input('Enter number of transmitted pulses:  ')
for M=1:209
        outsinc=fbark13(N,M);
        t=[1:length(outsinc)];
        outpsinc(M,t)=outsinc;
end
outpsinc=abs(outpsinc);
n=num2str(N);
mesh(-((length(outpsinc)/2)+1)/tau:1/tau:...     %PLOT AMB.FUNCTION
((length(outpsinc)/2)-2)/tau,...
-104/tau:1/tau:104/tau, outpsinc )
grid
view(45,30);
xlabel('lambda/tau')
ylabel('DELTA(phi)/tau')
title(['AMBIGUITY FUNCTION OF UWB BARKER-13 FOR N = ',n,''])
print bark13a
pause
contour(-((length(outpsinc)/2)+1)/tau:1/tau:...  %CONTOUR AMB.FUNCTION
((length(outpsinc)/2)-2)/tau,...
-104/tau:1/tau:104/tau, outpsinc )
grid
xlabel('lambda/tau')
ylabel('DELTA(phi)/tau')
title(['CONTOUR PLOTS OF UWB BARKER-13 AMBIGUITY FUNCTION FOR N = ',n,''])
print bark13b



function y=fbark13(N,M)
```

```
% THIS FUNCTION PRODUCES BARKER 13 UWB RADAR PULSES AND ALLOWS
% CORRELATES THEM AND TO PRODUCE OUTPUT FOR THE DOPPLER PROCESSOR

%************************************************************
%       THIS PROGRAM PRODUCES A SINGLE UWB BARKER-13 PULSE
%************************************************************

h=65;
Tb=65;
T=4*Tb;
tau=13*T/Tb;
t=0:1/Tb:4;
phi=25;
fo=0.25;
wo=2*pi*fo;
Vn=0;
A=1;
p=65;
for i=1:1:h
        Vi = (2*sin(10*i*pi/p)-2*sin(14*i*pi/p)+2*sin(18*i*pi/p)...
            -2*sin(20*i*pi/p)+2*sin(22*i*pi/p)-2*sin(24*i*pi/p)...
            +sin(26*i*pi/p))/i*cos(i*wo*t)...
            +(1-2*cos(10*i*pi/p)+2*cos(14*i*pi/p)-2*cos(18*i*pi/p)...
            +2*cos(20*i*pi/p)-2*cos(22*i*pi/p)+2*cos(24*i*pi/p)...
            -cos(26*i*pi/p))/i*sin(i*wo*t);

Vn=Vn+Vi;
end
V=(A/pi)*Vn;
subplot(2,1,1),
plot(t,V)                   %PLOT UWB BARKER-13 PULSE
grid
xlabel('Time/T')
ylabel('Normalized Amplitude')
title('UWB RADAR PULSE WITH BARKER CODE 13')

%************************************************************
%       THIS PROGRAM PRODUCES TRAIN OF N UWB BARKER-13 PULSES
%************************************************************

srN=[];
for n=1:N
        srN=[srN V];
end
trN=0:length(srN)-1;
trN=trN/T;
subplot(2,1,2)
plot(trN,srN)                   %PLOT N UWB BARKER-13 PULSES
grid
xlabel('Time/T')
```

```
ylabel('Normalized Amplitude')
title('TRAIN OF UWB RADAR PULSES WITH BARKER-13')
print fbark13a
pause

%************************************************************************
% THIS PROGRAM PRODUCES AUTOCORRELATION OF SINGLE UWB BARKER-13 PULSE
%************************************************************************

slidout=xcorr(Vn);
slidout=slidout';
slidout=slidout/max(slidout);
ts=0:length(slidout)-1;
ts=ts/T;
subplot(2,1,1)
plot(ts,slidout)              %PLOT AUTOCORRELATION UWB BARKER-13 PULSE
grid
xlabel('Time/T')
ylabel('Normalized Amplitude')
title('MATCHED FILTER OUTPUT OF UWB RADAR PULSE WITH BARKER-13')

%************************************************************************
%THIS PROGRAM PRODUCES AUTOCORRELATION TRAIN OF N UWB BARKER-13 PULSES
%************************************************************************

corrout=[];
for n=1:N
        corrout=[corrout slidout];
end
tc=0:length(corrout)-1;
tc=tc/T;
subplot(2,1,2),
plot(tc,corrout)              %PLOT AUTOCORRELATION N UWB BARKER-13 PULSES
grid
xlabel('Time/T')
ylabel('Normalized Amplitude')
title('MATCHED FILTER OUTPUT FOR TRAIN UWB PULSES WITH BARKER-13')
print fbark13b
pause

%*****************************************************************
% THIS PROGRAM PRODUCES OUTPUT OF DOPPLER PROCESSOR
%*****************************************************************

Doplrout=slidout;
input=slidout;
phiz=M;
for i=1:N-1
        input=[zeros(1,(phi)) input];
        feedout=[zeros(1,(phiz)) Doplrout];

        if phiz >= phi
```

```
            DopIrout=feedout+[input zeros(1,i*(phiz-phi))];
        else
            DopIrout=input+[feedout zeros(1,(phi-phiz))];

        end
end

procorout=DopIrout/N;
t=[0:length(procorout)-1];
t=t/tau;
plot(t,procorout)          %PLOT DOPPLER PROCESSOR OUTPUT
grid
xlabel('lambda/tau')
ylabel('Normalized Amplitude')
delta(phi)=num2str((phiz-phi)/tau)
gtext(['(delta(phi))= ',delta(phi),'T FOR UWB BARKER-13 SIGNAL (N=4)'])
print fbark13c
pause

y=procorout;
```

LIST OF REFERENCES

1. Skolnik, M.I., *An Introduction to Impulse Radar*, Naval Research Laboratory, Washington, DC, 1990, (pp. 1-45).

2. Davis, C., Tomljanovich, N., Kramer, J., Poirier, J., "Characteristics of Ultrawide Band Radars Pertinent to Air Defense," *Ultrawideband Radar. Proceedings of the First Los Alamos Symposium*, CRC Press, Inc., 1991, (pp. 501-503).

3. Morrys, G., *Airborne Pulse Doppler Radar*, Artech House, Inc. 1988, (p. 145).

4. Woodward, P. M., *Probability and Information Theory with Applications to Radar*, 1953.

5. Skolnik, M. I., *Introductic , to Radar Systems.* Mc. Graw-Hill. 1980. (pp 411-434)

6. Levanon, N., *Radar Principles*, John Wiley & Sons, 1988.

7. Kelly, E.J., and Wishner, R.P. "Matched-Filter Theory for High-Velocity, Accelerating Targets," *IEEE Transactions*, Vol. MIL-9. 1965.

8. Altes, R., "Methods of Wideband Signal Design for Radar and Sonar Systems." Ph.D Thesis, University of Rochester, Rochester, NY. 1970. (pp. 1-11).

9. Mohamed, N.J., Resolution Function of Non-sinusoidal Radar Signals I: Range-Velocity Resolution with Rectangular Pulses," *IEEE Transactions on Electromagnetic Compatibility* Vol .32. No. 2. May 1990. (pp. 153-160).

10. Mohamed, N.J., "Resolution Function of Non-sinusoidal Radar Signals II: Range-Velocity Resolution with Pulse Compression Techniques," *IEEE Transactions on Electromagnetic Compatibility*, Vol. 33. No. 1, February, 1991. (pp. 51-58).

11. Nathanson, F. E., *Radar Design Principles*, McGraw-Hill, 1969.

12. Berkowitz, R. S., *Modern Radar: Analysis, Evaluation and System Design*, John Wiley & Sons, Inc. 1965.

13. Cook, C. and Bernfeld, M. *Radar Signal: An Introduction to Theory and Application*, Academic Press Inc., 1967.

14. Brookner, E. *Radar Technology*, Artech House, Inc. 1978.

15. Harmuth, H.F., *Non Sinusoidal Waves for Radar and Radio Communication*, Academic Press Inc. New York, NY. 1981.

16. Tang, R., Lee, K., and Pusateri, V., "An Ultra Wideband Adaptive Transmitter for Ultra Wideband Radar Feasibility Demonstration," *Ultrawideband Radar Proceedings, SPIE*, Vol. 1631, 1992, (pp 127-133).

17. *MATLAB Reference Guide*, The Math Works, Inc. 1992.

INITIAL DISTRIBUTION LIST

1. Defense Technical Information Center — 2
   Cameron Station
   Alexandria, VA 22304-6145

2. Library, Code 52 — 2
   Naval Postgraduate School
   Monterey, CA 93943-5002

3. Chairman, Code EC — 1
   Department of Electrical and Computer Engineering
   Naval Postgraduate School
   Monterey, CA 93943-5002

4. Professor G. S. Gill, Code EC/Gl — 3
   Department of Electrical and Computer Engineering
   Naval Postgraduate School
   Monterey, CA 93943-5002

5. Professor Darwish Abdel Aziz Mohamed, — 1
   Air Defense College
   El Tabia, Alexandria
   Egypt

6. Escuela Superior de Guerra Naval — 1
   AV. Cuyuni, Colinas de Bello Monte,
   Caracas, 1041
   Venezuela

7. Escuela Naval de Venezuela — 1
   Director
   Comandancia General de la Armada
   Av. Vollmer San Bernardino
   Caracas, 1011
   Venezuela

8. Escuela de Postgrado de la Armada
   Director
   Comandancia General de la Armada
   Av. Vollmer San Bernardino
   Caracas, 1011
   Venezuela
   1

9. Direccion de Armamento y Electronica (DAE)
   Comandancia General de la Armada
   Av. Vollmer San Bernardino
   Caracas, 1011
   Venezuela
   1

10. CC Efrain Leon Guerra
    USMILGP Venezuela
    NAVSEC
    APO Miami 34037-0008
    2